Revised Version

DESY 01-076
TSL/ISV-2001-0250

arXiv:hep-ph/0106246 v2 4 Sep 2001

DESY 01-076
June 2001

Soft Color Interactions and Diffractive Hard Scattering at the Fermilab Tevatron

R. Enberg[a], G. Ingelman[ab], N. Tîmneanu[a]

[a] *High Energy Physics, Uppsala University, Box 535, S-751 21 Uppsala, Sweden*

[b] *Deutsches Elektronen-Synchrotron DESY, Notkestrasse 85, D-22603 Hamburg, Germany*

Abstract

An improved understanding of nonperturbative QCD can be obtained by the recently developed soft color interaction models. Their essence is the variation of color string-field topologies, giving a unified description of final states in high energy interactions, e.g., diffractive and nondiffractive events in ep and $p\bar{p}$. Here we present a detailed study of such models (the soft color interaction model and the generalized area law model) applied to $p\bar{p}$, considering also the general problem of the underlying event including beam particle remnants. With models tuned to HERA ep data, we find a good description also of Tevatron data on production of W, beauty and jets in diffractive events defined either by leading antiprotons or by one or two rapidity gaps in the forward or backward regions. We also give predictions for diffractive J/ψ production where the soft exchange mechanism produces both a gap and a color singlet $c\bar{c}$ state in the same event. This soft color interaction approach is also compared with Pomeron-based models for diffraction, and some possibilities to experimentally discriminate between these different approaches are discussed.

12.38.Lg, 12.38.Aw

Typeset using REVTEX

I. INTRODUCTION

A major unsolved problem in particle physics is to understand strong interaction processes with a small ('soft') momentum transfer. The most striking illustration of this is the confinement of quarks and gluons in hadrons and the related hadronization process giving the observable hadronic final states in high energy collisions. In terms of Quantum Chromodynamics (QCD), small momentum transfers have a large coupling α_s such that a perturbative expansion in terms proportional to powers of α_s^n does not work. This is in contrast to processes with a 'hard' scale, i.e., a large momentum transfer, where α_s is small and perturbative QCD (pQCD) on the level of quarks and gluons works well. To gain understanding of soft, nonperturbative QCD (non-pQCD) it is therefore advantageous to first consider soft effects in hard scattering events, since the hard scale gives a firm ground in terms of a parton level process which is calculable in pQCD. This hard-soft interplay is the basis for the topical research field of diffractive hard scattering [1].

Diffractive events can be characterized by having a rapidity gap, i.e., a region in rapidity (or polar angle) without any particles. Another definition is to require a leading particle carrying most of the beam particle momentum ($x_F \gtrsim 0.9$), which is kinematically related to a rapidity gap. These rapidity gaps in the forward or backward rapidity regions, connect to the soft part of the event and therefore nonperturbative effects on a long space-time scale are certainly important. The central rapidity gaps between high-$p_\perp$ jets, observed at the Tevatron [2], may be of a different kind since the hard momentum transfer is across the gap. This gap phenomenon will therefore not be considered here, but is studied separately [3].

Diffractive scattering has traditionally been explained in the Regge framework by the exchange of a Pomeron [4]. For processes with a hard scale, a parton structure of the Pomeron may be considered [5]. With the Pomeron flux given by Regge phenomenology, the HERA data on diffractive deep inelastic scattering can be well described by fitting parton density functions in the Pomeron [6,7]. However, applying exactly the same model for $p\bar{p}$ gives a too large cross section for diffractive hard processes. Compared to the Tevatron data in Table I, such a Pomeron model gives about a factor six too large rates of W and dijets with one gap and two orders of magnitude too large rates of dijets with two gaps [8]. This is related to the failure of the factorization theorem for hard diffractive hadron-hadron scattering, although it holds in diffractive deep inelastic scattering (DIS) [9]. It is also an indication of a non-universality problem of the Pomeron model, which may be related to the Pomeron flux. Since this flux specifies the leading particle spectrum, it is interesting to note that the new Tevatron data [10] with a leading antiproton show a similar problem of the Pomeron model. These problems of the Pomeron approach are further discussed in Section II.

In order to better understand nonperturbative dynamics and to provide a unified description of all final states, the soft color interaction (SCI) model [11,12] and the generalized area law (GAL) model [13] were developed. These are added to Monte Carlo generators (LEPTO [14] for ep and PYTHIA [15] for $p\bar{p}$) which simulate the interaction dynamics and provide a complete final state of observable particles, such that an experimental approach can be taken to classify events depending on the characteristics of the final state: e.g., gaps or no-gaps, leading protons or neutrons, etc.

The basic assumption of the models is that variations in the topology of the confining

TABLE I. Ratios diffractive/inclusive for hard scattering processes in $p\bar{p}$ collisions at the Tevatron, showing experimental results from CDF and D0 compared to the SCI and GAL soft color exchange models.

Observable	$\sqrt{s}$		Ratio [%]		
	[GeV]	Experiment	Observed	SCI	GAL
W - gap	1800	CDF [17]	1.15 ± 0.55	1.2	0.8
Z - gap	1800	—	—[a]	1.0	0.5
$b\bar{b}$ - gap	1800	CDF [18]	0.62 ± 0.25	0.7	1.4
J/ψ - gap	1800	—	—[a]	1-2[b]	1-2[b]
jj - gap	1800	CDF [19]	0.75 ± 0.10	0.7	0.6
jj - gap	1800	DØ [20]	0.65 ± 0.04	0.7	0.6
jj - gap	630	DØ [20]	1.19 ± 0.08	0.9	1.2
gap - jj -gap[c]	1800	CDF [21]	0.26 ± 0.06	0.2	0.1
$\bar{p}$ - jj -gap[c]	1800	CDF [22]	0.80 ± 0.26	0.5	0.4

[a] No result available

[b] Depending on kinematical requirements for J/ψ

[c] Ratio of two-gap events to one-gap events

color force fields (strings [16]) lead to different hadronic final states after hadronization. The pQCD interaction gives a set of partons with a specific color order. However, this order may change owing to soft, nonperturbative interactions. The details of our models for such interactions are described in Section III. One may at first think that this approach is some kind of model for the Pomeron. To the extent that the term 'Pomeron' is associated with the Regge approach, this is not the case since nothing from the Regge formalism is being used or referred to. The soft color interaction models also give quite different results when applied to diffractive hard scattering at the Tevatron. An overall summary of the relative rates of various diffractive hard processes is given in Table I, which shows that this approach can account for several different gap phenomena (taking the uncertainty in models and data into account). The details of this and other results are presented and discussed in Sections IV, V and VI.

As opposed to the standard Pomeron approach, the SCI and GAL models can describe diffractive events both at HERA and at the Tevatron. This is not achieved by introducing several free parameters. On the contrary, the models have essentially only *one* new parameter to account for the unknown nonperturbative dynamics. This parameter is determined from the HERA data on the diffractive structure function F_2^D [7] and then used with the same computer code implemented in PYTHIA to simulate $p\bar{p}$ at the Tevatron.

The SCI and GAL models are very general in that they are able to describe a large set of different data. This does not only refer to diffraction, but also various nondiffractive observables. Particularly noteworthy is that the SCI model reproduces the observed rate of high-$p_\perp$ charmonium and bottomonium at the Tevatron [23], which is factors of 10 larger than the predictions based on the color singlet model in conventional pQCD. Although the SCI and GAL models are too simple and have too weak theoretical content to provide a satisfactory understanding, their general applicability and success in describing different

kinds of observables show that different phenomena may have a common explanation. They represent a new approach which, together with others mentioned in the Conclusions, may lead us towards a proper understanding of nonperturbative QCD.

II. POMERON PROBLEMS

The inability to describe both HERA and $p\bar{p}$ collider data on hard diffraction is a problem for the Pomeron model. It shows that the 'standard' Pomeron flux factor [24],

$$f_{I\!P/p}(x_{I\!P},t) = \frac{9\beta_0^2}{4\pi^2}\left(\frac{1}{x_{I\!P}}\right)^{2\alpha_{I\!P}(t)-1}[F_1(t)]^2 \qquad (1)$$

and Pomeron parton densities, $f_{i/I\!P}(x,Q^2)$, cannot be used universally. This flux is found to give a much larger cross section for inclusive single diffraction than measured at $p\bar{p}$ colliders, although it works well for lower energy data. This is due to the increase of the flux as the minimum $x_{I\!P\,min} = M^2_{X\,min}/s$ gets smaller with increasing cms energy $\sqrt{s}$. To avoid this unphysical increase, a Pomeron flux 'renormalization' has been proposed [25] by enforcing that the integral of the flux saturates at unity (by dividing by the integral whenever it is larger than unity). This prescription not only gives the correct inclusive single diffractive cross section at collider energies, but it also makes the HERA and Tevatron data on hard diffraction compatible with the Pomeron hard scattering model. The model result for HERA is not affected, but at the higher energy of the Tevatron the Pomeron flux is reduced such that the data are essentially reproduced. In another proposal [26] based on an analysis of single diffraction cross sections, the Pomeron flux is reduced at small $x_{I\!P}$ through an $x_{I\!P}$- and t-dependent damping factor. The pros and cons of these two approaches to modify the Pomeron flux have been debated.

It has recently been shown [27] that the Tevatron data on diffractive W production can be reproduced if a harder Pomeron flux is introduced together with a Pomeron intercept higher than the value extracted from HERA data. These changes from the conventional Pomeron model illustrate the problem of having a universally applicable Pomeron model. In a proposed new phenomenological approach [28] the structure of the Pomeron is derived from that of the parent proton such that the gap probability is obtained from the soft parton density at $x_{I\!P}$. Some general features of diffractive DIS are obtained, but a more detailed confrontation with data remains to be performed.

A difference between diffraction in ep and $p\bar{p}$ is the possibility for coherent Pomeron interactions in the latter [29]. In the incoherent interaction only one parton from the Pomeron participates and any others are spectators. However, in the Pomeron-proton interaction with $I\!P = gg$ both gluons may take part in the hard interaction giving a coherent interaction. For example, in the $I\!Pp$ hard scattering subprocess $gg \to q\bar{q}$, the second gluon from the Pomeron may couple to the gluon from the proton. Such diagrams cancel when summing over all final states for the inclusive hard scattering cross section (the factorization theorem). For gap events, however, the sum is not over all final states and the cancellation fails leading to factorization breaking for these coherent interactions where the whole Pomeron momentum goes into the hard scattering system. This coherent interaction cannot occur in the same way in deep inelastic scattering (DIS) since the Pomeron interacts with a particle

without colored constituents. This difference between ep and $p\bar{p}$ means that there should be no complete universality of parton densities in the Pomeron. The difference between diffractive hard scattering at HERA and the Tevatron can be described in terms of an overall suppression factor or gap 'survival probability', due to extra soft rescattering effects in $p\bar{p}$, estimated using an eikonal model [30].

Although modified Pomeron models may describe the rapidity gap events reasonably well, there is no satisfactory understanding of the Pomeron and its interaction mechanisms. On the contrary, there are conceptual and theoretical problems with this framework. The Pomeron is not a real state, but only a virtual exchanged spacelike object. The concept of a structure function is then not well defined and, in particular, it is unclear whether a momentum sum rule should apply. In fact, the factorization into a Pomeron flux and a Pomeron structure function cannot be uniquely defined since only the product is an observable quantity [31].

It may therefore be improper to regard the Pomeron as being 'emitted' by the proton, having QCD evolution as a separate entity and being 'decoupled' from the proton during and after the hard scattering. Since the Pomeron-proton interaction is soft, its time scale is long compared to the short space-time scale of the hard interaction. It is therefore natural to expect soft interactions between the Pomeron system and the proton both before and after the snapshot of the high-Q^2 probe provided by the hard scattering. The Pomeron can then not be viewed as decoupled from the proton and, in particular, is not a separate part of the QCD evolution in the proton.

Large efforts have been made to understand the Pomeron as a two-gluon system or a gluon ladder in pQCD. By going to the soft limit one may then hope to gain understanding of non-pQCD and, perhaps, establish a connection between pQCD in the small-x limit and Regge theory. More explicitly, diffractive DIS has been considered in terms of models based on two-gluon exchange in pQCD, see e.g. [32]. The basic idea is to take two gluons in a color singlet state from the proton and couple them to the $q\bar{q}$ system from the virtual photon. With higher orders included the diagrams and calculations become quite involved. Nevertheless, these approaches can be made to describe the main features of the diffractive DIS data. Although this illustrates the possibilities of the pQCD approach to the Pomeron, one is still forced to include nonperturbative modeling to connect the two gluons in a soft vertex to the proton which goes beyond the conventional use of parton densities. Thus, even if one can gain understanding by working as far as possible in pQCD, one cannot escape the fundamental problem of understanding non-pQCD.

III. MODELS FOR SOFT COLOR INTERACTIONS

Given these practical and conceptual problems of the Regge-based Pomeron model and the impossibility to cover all important aspects by a pQCD treatment, new approaches should be investigated. We are here exploring new ideas to model non-pQCD interactions, which avoid the concept of a Pomeron and provide a single simple model that describes all final states, with or without rapidity gaps.

The starting point is that the hadronic final state is produced through the hadronization of partons emerging from a hard scattering process which can be well described by pQCD.

The basic new idea is that there may be additional soft color interactions at a scale below the cutoff Q_0^2 for the perturbative treatment. Obviously, interactions will not disappear below this cutoff. On the contrary, they will be abundant due to the large coupling α_s at small scales. The question is rather how to describe these interactions properly. Here, we introduce soft color interactions which do not change the dynamics of the hard scattering, but change the color topology of the state such that another hadronic final state emerges after hadronization. This topology can be described in terms of color triplet strings and the standard Lund model [16] can be used for a well established treatment of the hadronization of any given string configuration. We have tried two different ways to model the soft exchange of color-anticolor representing nonperturbative gluon exchange. The soft color interaction model is formulated in a parton basis with color exchanges between the partons emerging from the hard scattering process (including remnants of initial hadrons). The generalized area law model is instead formulated in a string basis, since strings are here assumed to be the proper states for soft exchanges that may not resolve partons. In spite of this difference, the models have a very similar structure and may be regarded as variations on the same general theme.

The SCI and GAL models are constructed as subroutines added to the Monte Carlo event generators LEPTO [14] for ep and PYTHIA [15] for $p\bar{p}$. This gives powerful tools for detailed investigations of the models and their ability to reproduce experimental data.

Since the soft non-pQCD processes cannot alter the hard perturbative scattering processes, the latter should be kept unchanged in the models. Therefore, the hard parton level interactions are treated in the normal way using standard hard scattering matrix elements (electroweak or QCD) plus initial and final state parton showers based on the DGLAP leading logarithm evolution equations [33] to simulate higher order pQCD processes. Thus, the set of partons, including those in beam hadron remnants, are generated as in conventional ep and $p\bar{p}$ hard scattering processes. The SCI and GAL models are then added as an extra intermediate step before the hadronization is performed using the Lund Monte Carlo JETSET [15].

In this section we first describe these two models in some detail and then discuss other aspects of soft interactions which are common for both models and must be considered in a complete Monte Carlo model.

A. The SCI model

The soft color interaction (SCI) model [11,12] is applied to the parton state emerging from the hard scattering. It gives the possibility for each pair of these color charged partons to make a soft interaction. One may here include all possible pairs of partons or require that one parton belongs to the remnant. In the latter case, one may view this as the perturbatively produced quarks and gluons interacting softly with the color medium of the proton as they propagate through it. The soft interaction changes only the color but not the momentum and may be viewed as soft nonperturbative gluon exchange. This should be a natural part of the process in which bare perturbative partons are dressed into nonperturbative ones and the formation of the confining color flux tube in between them. This necessarily involves some, not yet understood nonperturbative interactions which the model attempts to describe.

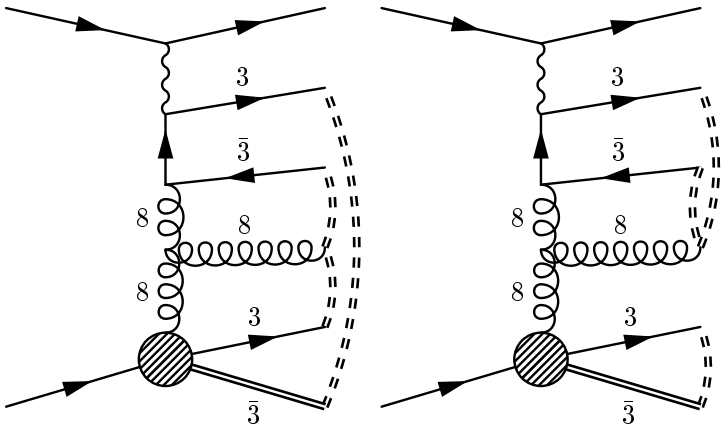

FIG. 1. Boson-gluon fusion process in DIS with string configuration (double-dashed line) in (left) the conventional Lund string model connection of partons and (right) after a soft color octet exchange between the remnant and the hard scattering system as modeled by SCI or GAL resulting in a phase space region without a string leading to a rapidity gap event after hadronization.

Being a nonperturbative process, the exchange probability cannot presently be calculated and is therefore described by a phenomenological parameter P. The number of soft exchanges will vary event-by-event and change the color topology such that, in some cases, color singlet subsystems arise separated in rapidity, as illustrated Fig. 1 where, e.g., a color exchange between the perturbatively produced quark and the quark in the remnant has taken place. Color exchanges between the perturbatively produced partons and the partons in the proton remnant (representing the color field of the proton) are of particular importance for the gap formation. It should be emphasized, however, that the model is quite general giving rise to events both with and without rapidity gaps.

Since DIS is a simpler and cleaner process than $p\bar{p}$ collisions, the model was first developed for DIS and successfully tested against diffractive DIS data from HERA [11,12,34]. The rate and main properties of the gap events are qualitatively reproduced. The rate of gap events depends on the parameter P, but the dependence is not strong giving a stable model with $P \simeq 0.2$–0.5. This color exchange probability is the only new parameter in the model. Other parameters belong to the conventional LEPTO model [14] and have their usual values. The rate and size of gaps do, however, depend on the amount of parton emission. In particular, more initial state parton shower emissions will tend to populate the forward rapidity region and prevent gap formation [12].

The gap events show the properties characteristic of diffraction. The exponential t-dependence arises in the model from the intrinsic transverse momentum (Fermi motion) of the interacting parton which is balanced by the proton remnant system. This remnant gives rise to leading protons with a peak at large fractional momentum x_F, as well as proton dissociation.

The salient features of the measured diffractive structure function are also reproduced [34]. The behavior of the data on $F_2^D(\beta, Q^2)$ is in the SCI model understood as normal

pQCD evolution in the proton. The rise with $\ln Q^2$ also at larger β is simply the normal behavior at the small momentum fraction $x = \beta x_{I\!P}$ of the parton in the proton. Here, $x_{I\!P} = \frac{Q^2+M_X^2-t}{Q^2+W^2-m_p^2} \approx \frac{x(Q^2+M_X^2)}{Q^2}$ is only an extra variable related to the gap size or M_X, which does not require a Pomeron interpretation. The flat β-dependence of $x_{I\!P}F_2^D = \frac{x}{\beta}F_2^D$ is due to the factor x compensating the well-known increase at small-x of the proton structure function F_2.

This Monte Carlo model gives a general description of DIS, with and without gaps. In fact, it can give a fair account of such 'orthogonal' observables as rapidity gaps and the large forward E_T flow [12]. Diffractive events are in this model defined through the topology of the final state, in terms of rapidity gaps or leading protons just as in experiments. There is no particular theoretical mechanism or description in a separate model, like Pomeron exchange, that defines what is labeled as diffraction. This provides a smooth transition between diffractive gap events and nondiffractive (no-gap) events [35]. In addition, leading neutrons are also obtained in fair agreement with recent experimental measurements [36]. In a conventional Regge-based approach, Pomeron exchange would be used to get diffraction, pion exchange added to get leading neutrons and still other exchanges added to get a smooth transition to normal DIS. The SCI model demonstrates that a simpler theoretical description can be obtained.

B. The GAL model

The generalized area law (GAL) model [13] for color string re-interactions is a model for soft color exchanges which is similar in spirit to the SCI model. Whereas the SCI model is formulated as soft exchanges between the partons emerging from the hard scattering process, the GAL model is formulated in terms of interactions between the strings connecting these partons. Soft color exchanges between strings change the color topology resulting in another string configuration, as illustrated in Fig. 1.

The probability for two strings to interact is in the GAL model obtained as a generalization of the area law suppression e^{-bA} with the area A swept out by a string in energy-momentum space. The model uses the measure $A_{ij} = (p_i + p_j)^2 - (m_i + m_j)^2$ for the piece of string between two partons i and j. This results in the probability $P = P_0[1 - \exp(-b\Delta A)]$ depending on the change ΔA of the areas spanned by the strings in the two alternative configurations of the strings, i.e., with or without the topology-changing soft color exchange. The exponential factor favors making 'shorter' strings, e.g., events with gaps, whereas making 'longer' strings is suppressed. The fixed probability for soft color exchange in SCI is thus in GAL replaced by a dynamically varying one.

There is only one new parameter in the GAL model, i.e., P_0 instead of P in SCI. b is one of the usual hadronization parameters in the Lund model [16], but its value must be retuned when changing the string configuration. Since the GAL model is formulated in terms of strings, it should be applicable to all interactions producing strings, i.e., also to hadronic final states in e^+e^-. The parameter values used in the GAL model were obtained [13] by making a simultaneous tuning to the diffractive structure function in DIS and the charged particle multiplicity distribution and momentum distribution for $\pi^\pm$ in e^+e^- annihilation at the Z^0-resonance. This resulted in $P_0 = 0.1$, $b = 0.45$ GeV^{-2} and $Q_0 = 2$ GeV, where

Q_0 is the cutoff for initial and final state parton showers. It is not possible to have the JETSET default cutoff $Q_0 = 1$ GeV in the parton showers and simultaneously reproduce the multiplicity distribution. One might worry that the obtained cutoff is relatively large compared to the default value. However, it is not obvious that perturbation theory should be valid for so small scales when more exclusive final states are considered. Therefore, Q_0 can be seen as as a free parameter describing the boundary below which it is more fruitful to describe the fragmentation process in terms of strings instead of perturbative partons.

With this parameter tuning the GAL model gives very similar results [13] for the final state in $e^+e^- \to Z^0 \to hadrons$ as default JETSET. This concerns multiplicity distributions, momentum distributions and string effects. Also the conventional rapidity gap behavior is obtained, i.e., an exponentially falling distribution with increasing size Δy of the largest rapidity gap in the event.

Applying the GAL model to DIS at HERA [34] gives a quite good description of the diffractive structure function $F_2^{D(3)}(x_{I\!P}, \beta, Q^2)$ observed by H1. The details at low Q^2 is actually better reproduced with GAL than with SCI. The GAL model cures the problem the SCI model has in producing somewhat too many soft hadrons in inclusive DIS, but results in too low transverse energy flow in the forward region. These effects are related to events where the string after SCI goes back-and-forth producing a zig-zag shape, i.e., a longer string, giving more but softer hadrons after hadronization. Conversely, the GAL model suppresses topologies with long strings.

C. Remnants and soft underlying event

To obtain a complete model for the production of the observable hadronic final state there are further issues of nonperturbative dynamics that have to be considered. These include not only the hadronization process itself, but also the treatment of remnants of the colliding hadrons and possible additional dynamics in order to achieve a decent description of the soft underlying event, i.e., underlying the hard scattering part of the event. Here, we essentially use the standard models developed for the family of Lund Monte Carlo programs, but with some modifications and further developments as will be described in this subsection.

The standard Lund hadronization model [16] as implemented in JETSET [15] is used for the formation of hadrons from color triplet string fields. However, the final state will depend on how the strings are stretched between partons, as exemplified by the SCI and GAL models above. Similarly, the resulting string system will depend on how the hadron remnants are treated and if additional strings are formed, e.g., to produce additional hadronic activity in the underlying event.

The remnant system is the initial (anti)proton 'minus' the parton entering the hard scattering process, i.e., the hard $2 \to 2$ scattering given by matrix elements combined with parton showers. The initial parton carries a momentum fraction x_0 of the beam proton as given by the parton density distributions $f_i(x_0, Q_0^2)$ at the scale Q_0^2 where the initial state parton shower is terminated in its backwards evolution simulation. This leaves the fraction $1 - x_0$ for the proton remnant system. The initial parton can be either a valence quark, a sea quark or a gluon. In case a valence quark is removed from the initial proton, the remnant is a diquark with an anti-triplet color charge that defines the endpoint of a triplet

string. If the initial parton is a gluon, the remnant contains all three valence quarks in a color octet state which is split into a color triplet quark and a color anti-triplet diquark that form the end-points on two triplet strings. Here, the quark and diquark share the remnant momentum in the fractions χ and $1-\chi$, respectively, as given by parametrizations of $\mathcal{P}(\chi)$ in PYTHIA and to be further discussed below.

In case a sea quark is removed from the initial proton, the remnant system is more complex, containing all three valence quarks plus the partner of the interacting sea quark in order to conserve quantum numbers. Here, a more elaborate sea quark treatment (SQT) has been introduced [14,12]. The interacting quark, with flavor and momentum x_0 obtained from the initial state parton shower evolution, is taken as a valence or sea quark based on the relative sizes of the corresponding parton distributions $q_{val}(x_0, Q_0^2)$ and $q_{sea}(x_0, Q_0^2)$. In case of a sea quark, the left-over partner is given an explicit momentum. Here, we have tried two possibilities to model this unknown dynamics. In the first (SQT1), the longitudinal momentum fraction is given by the Altarelli-Parisi splitting function $P(g \to q\bar{q})$, i.e., the pQCD initial state parton shower routine is used to model a $g \to q\bar{q}$ process which is strictly speaking below the original parton shower cutoff. As an alternative (SQT2) the sea quark partner is assigned a longitudinal momentum chosen from the corresponding sea quark momentum distribution in the proton. In both cases the transverse momentum is chosen from the same Gaussian used for the primordial transverse (Fermi) momentum. These two methods give similar results, but differ in some details as will be discussed below. The sea quark partner and the three valence quarks, which are split into a quark and a diquark as described, define the dynamics of the remnant system. These three color (anti)triplet objects in the remnants are then end-points on strings, implying additional string topology possibilities. Since the sea quark partner has only a small transverse momentum, it affects in particular the very forward part of the final hadronic state. Therefore, it is of interest for the formation of rapidity gaps studied here.

A related issue is the treatment of a color singlet system (string) with small invariant mass. The Lund hadronization model is constructed for large mass strings, but can be applied to systems of invariant mass which is as low as the sum of the end-point parton masses plus an additional ~ 1 GeV. When the string mass is so small that only one or two hadrons can be formed, normal string hadronization is not applicable since energy-momentum constraints and resonance phenomena demand special treatment. This is instead achieved through the new routines (LSMALL in LEPTO and PYSMALL in PYTHIA). Of particular importance for the investigations in this paper is the formation of a single leading proton (or antiproton) giving the diffractive signature. The mapping of a string with a continuous mass distribution onto a particular on-shell hadron with fixed mass, requires a shuffling of energy-momentum to another string system in order to conserve energy-momentum in the event [15]. By transferring the required energy-momentum to/from another parton which is as far away as possible in phase space, the relative disturbance on the four-vectors is kept minimal and typically of order tens of MeV, i.e., small even on the hadronization momentum transfer scale.

Starting with the hard scattering processes (matrix elements and parton showers) and adding this remnant treatment followed by Lund string model hadronization results in a Monte Carlo event generator producing a complete hadronic final state. The resulting hadronic activity is, however, too small compared to collider data [37]. The observed mul-

tiplicities are larger, with the multiplicity distribution extending in a longer tail to large multiplicities. Furthermore, the number of particles per unit rapidity is larger and gives a higher rapidity plateau or 'pedestal' below high-$p_\perp$ jets than obtained in the model. This additional activity in the underlying event is related to soft QCD processes and is therefore difficult to describe in a theoretically satisfactory way.

In PYTHIA this additional activity in the underlying event is achieved by a model for multiple interactions (MI) [37,15]. This is constructed based on multiple parton-parton scatterings described by the QCD $2 \to 2$ matrix elements. At small momentum transfers this cross section becomes large, even larger than the $p\bar{p}$ total cross section which is interpreted as having more than one such parton-parton scattering in the same event. These scatterings can sometimes be hard enough to contribute to the rate of low-$p_\perp$ jets and minijets, but dominantly they have too small $p_\perp$ to give observable jet structure. These small-$p_\perp$ partons will stretch additional strings that produce more hadrons over large rapidity regions and thereby contribute substantially to the underlying event.

The cross section for these multiple scatterings diverge when the scattered parton $p_\perp \to 0$. This is avoided by some (arbitrary) regularization or a cutoff on $p_\perp$, which will be the main regulator of the amount of multiple scatterings that are generated. In the default version of the MI model in PYTHIA 5.7 a sharp cutoff $p_\perp^{\min} = 1.4$ GeV is used, although more complicated alternatives are available as options [15]. Using this MI model, data on multiplicities, rapidity distributions and pedestal effects at the S$p\bar{p}$S ($\sqrt{s} = 540$ and 630 GeV) [38] can be reasonably described [37]. Measurements of this kind have only recently been made at the Tevatron and the model has not yet been tested or tuned at the energy of interest in our study.

Although the MI model is based on pQCD parton-parton scattering, in this context the model is used to emulate soft nonperturbative effects. The soft color exchange models are also introduced to account for soft effects on the hadronic final state. The SCI model, in particular, can give zig-zag shaped strings which produce a larger number of hadrons per unit rapidity, i.e., more activity in the underlying event. There is therefore a risk of 'double counting' the soft effects and producing too much underlying soft activity if the SCI/GAL model and the MI model are simply added. With the SCI/GAL model tuned to data on rapidity gaps, we therefore lower the amount of multiple interactions by increasing the $p_\perp^{\min}$ parameter. This means that the pQCD-based MI model is not pushed to generate the softest dynamics, which is instead treated by the soft exchange models. We have studied this issue in some detail by looking at jet profiles, rapidity plateaus and charged particle multiplicities obtained by running PYTHIA with SCI/GAL added and the default MI model. Keeping the default value of $p_\perp^{\min}$ gives, as expected, too much underlying event activity, whereas increasing to $p_\perp^{\min} = 2.5$ GeV for SCI and to $p_\perp^{\min} = 2.0$ GeV for GAL, one obtains essentially the same results as default PYTHIA, and thereby reproduce data equally well. The lower value for the GAL model reflects the fact that longer strings are suppressed, and therefore GAL contributes less to the underlying event activity than SCI. We note that in the recently released version 6 of PYTHIA [39], the MI cutoff has been made energy dependent giving the value $p_\perp^{\min} = 2.1$ GeV at the Tevatron, i.e., closer to our values and indicating that the GAL model adds very little activity to the underlying event. Our $p_\perp^{\min}$ values have also been obtained by comparing with the diffractive data studied in this paper, but this will be discussed further below.

The sensitivity of our results to variations in these details of the modeling of the remnant and the underlying event has been investigated and is discussed below in connection with the comparison of our models and the available data.

IV. SINGLE DIFFRACTIVE HARD SCATTERING

Before discussing the details of how the SCI and GAL models apply in different single diffractive hard scattering processes in the following subsections, we first discuss some general aspects.

Single diffractive scattering is characterized by a large rapidity gap in the forward or backward hemisphere of a $p\bar{p}$ collision. The occurrence of rapidity gaps is very strongly affected by soft effects, as demonstrated in Fig. 2 for the case of diffractive W production. At the parton level, arising from the hard processes described by matrix elements and parton showers, there can be large regions of phase space where no partons have been emitted and thereby no strong suppression of the probability for large rapidity gaps. The partons are, however, connected by color force fields which through hadronization produce hadrons which fill these gaps in the final state. Thus, applying hadronization using the standard Lund string model, causes the drastic transition from the dashed to the dash-dotted curve in Fig. 2 such that large rapidity gaps in the final state of hadrons become exponentially suppressed. An extreme case is provided by the peak in the parton level curve, which arises from events where the W is produced by valence quark annihilation without parton radiation resulting in a huge rapidity separation between the two remnant systems (diquarks). Hadronization of the color string between these remnants produce hadrons in the full rapidity range, leaving no trace of the parton level gap.

This very strong effect of hadronization implies that modifications of the modeling of the poorly known nonperturbative QCD processes can have substantial effects. Applying the SCI model of last section, leads to an increased probability for large rapidity gaps (full curve in Fig. 2) at the hadron level, but still far below the parton level result. This difference relative to default PYTHIA may at first seem small, but for large gaps it is exactly what is needed to describe data as will be discussed in detail below. One may worry that there is no flat region, i.e., where the probability does not decrease with increasing gap size, which is sometimes taken as a characteristic for diffraction. This is due to the kinematical restriction on high-x_F leading protons imposed by the large W mass, as verified in the Monte Carlo by lowering m_W resulting in the expected diffractive behavior shown by the dotted curve in Fig. 2.

Diffractive events can be defined experimentally in two different ways: by a rapidity gap or by a leading (anti)proton. (Given the symmetry between proton and antiproton beams at the Tevatron, we usually mean either proton or antiproton when speaking of a leading proton.) The two methods are related, since kinematics requires an event with a leading proton to also have a gap. This has been explicitly investigated with our Monte Carlo model resulting in Fig. 3. Events with a very large gap do typically have a leading proton. At Tevatron energies, however, gaps of substantial size are kinematically allowed also for protons with not so high x_F as shown by the nontrivial correlations in Fig. 3b and c. This calls for some caution when comparing results based on these two definitions of

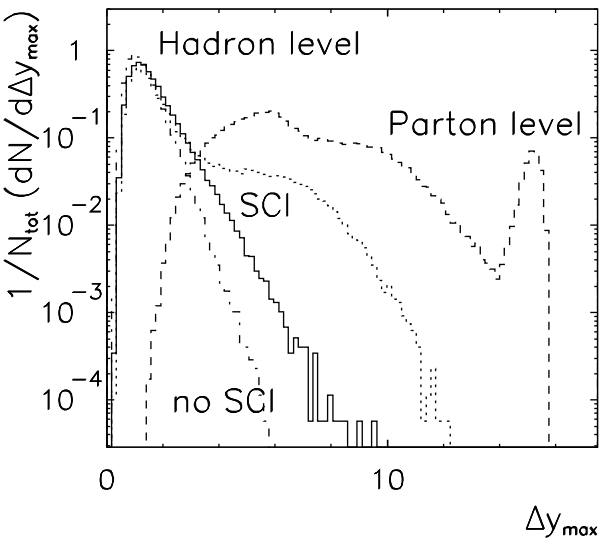

FIG. 2. Distribution of the size Δy_{max} of the largest rapidity gap in W production in $p\bar{p}$ events at $\sqrt{s} = 1.8$ TeV in PYTHIA. The dashed curve represents the parton level obtained from hard, perturbative processes. The dash-dotted curve is for the hadronic final state after standard hadronization, whereas adding the soft color interaction model results in the full curve and the dotted curve when setting $m_W = 8$ GeV to show the appearance of a 'diffractive plateau' when the kinematical constraint of the W mass is relaxed.

diffractive events. Irrespectively of this warning, comparing Fig. 3b and c shows the effect of the SCI model to produce more events with large-x_F protons and large gaps. When the leading proton is at a low x_F there may be another leading system of small invariant mass, in particular a large-x_F neutron. In addition to the events included in Fig. 3b and c, there is a substantial amount of gap events without a proton, but with other leading particles. Such events, which are natural products of the Monte Carlo model, must be included when using a gap definition of diffraction. The diffractive rates obtained with a gap definition are therefore usually larger than those obtained with a leading proton definition.

The experimental results on diffractive hard scattering processes have mainly been presented as relative rates, i.e., the cross section for a diffractive process divided by the total cross section for the same hard process. We denote this diffractive ratio by $R_{\rm hard}$, where 'hard' stands for the relevant hard subprocess. The first experimental analyses, e.g. [17–19], used a gap definition of diffraction. This is, however, essentially equivalent to requiring a leading proton with $x_F > 0.9$, such that the diffractive ratio $R_{\rm hard}$ can be expressed as

$$R_{\rm hard} = \frac{1}{\sigma^{\rm tot}_{\rm hard}} \int_{x_{F\,\rm min}}^{1} dx_F \, \frac{d\sigma_{\rm hard}}{dx_F}. \qquad (2)$$

where $x_{F\,\rm min}$ is the minimum leading proton x_F for an event to be considered diffractive. The

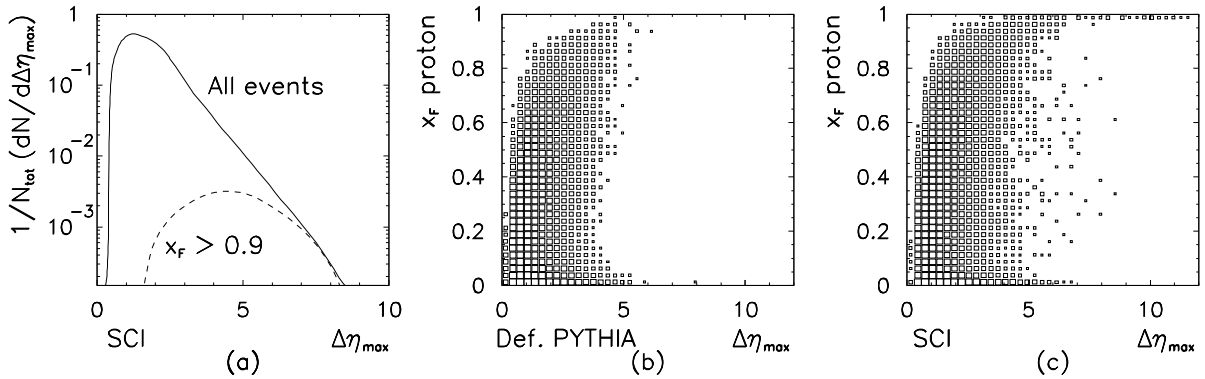

FIG. 3. Illustrations of the relation between the size $\Delta\eta_{max}$ of the largest rapidity gap and the momentum fraction x_F of the leading proton in simulated $p\bar{p}$ events at $\sqrt{s} = 1.8$ TeV. (a) Distribution of largest gap for all W events (full curve) in the SCI model and for the subsample having a leading proton with $x_F > 0.9$ (dashed). (b,c) Scatterplot (logarithmic scale) showing the correlation between leading proton x_F and associated largest gap for dijet production in (b) default PYTHIA and (c) when including the SCI model.

values of $R_{\rm hard}$ in Table I were obtained with $x_{F\rm min} = 0.9$, corresponding to the experimental analyses. This is also in accordance with the conventional definition of diffraction in the Regge approach and comparisons with simulations of Pomeron exchange at $x_{I\!P} = 1 - x_F < 0.1$ were made, leading to the problems discussed in Section II. The variation of $R_{\rm hard}$ with $x_{F\rm min}$ in the models will be discussed below.

Some more recent CDF analyses [10,22] could define diffraction through leading antiprotons observed in Roman pot detectors. This provided additional information, on $x_{I\!P}$ and the momentum fraction x of the struck parton in the incoming antiproton, making the results less inclusive. This gives additional handles to test the models, as will be discussed below.

Our results presented below were obtained by Monte Carlo simulations using PYTHIA version 5.7. As a reference, called 'default', we use standard PYTHIA with all parameters and switches at their default values. The parton distributions CTEQ3L [40] were used for the simulations with default PYTHIA and with the SCI model, and CTEQ4L [41] were used with GAL. There is a slight variation of the results depending on this choice, see Table II and the discussion in section IV A. The SCI and GAL models are simulated using added subroutines as described in Section III. This includes the improved procedures for beam particle remnants, with the treatment of sea quark interactions and small mass string systems.

In order to compare with the Pomeron model, we have also included results from simulations using the POMPYT program (version 2.6) [42]. Here, the Donnachie-Landshoff (DL) [24] Pomeron flux and the Gehrmann-Stirling (GS) [43] Pomeron structure functions were used. The GS parametrizations have two variants, referred to as model I and II. In short, model I describes the Pomeron as a hadronic system of quarks and gluons. Model II has, apart from this 'resolved' component, also a 'direct' component with a photon-Pomeron

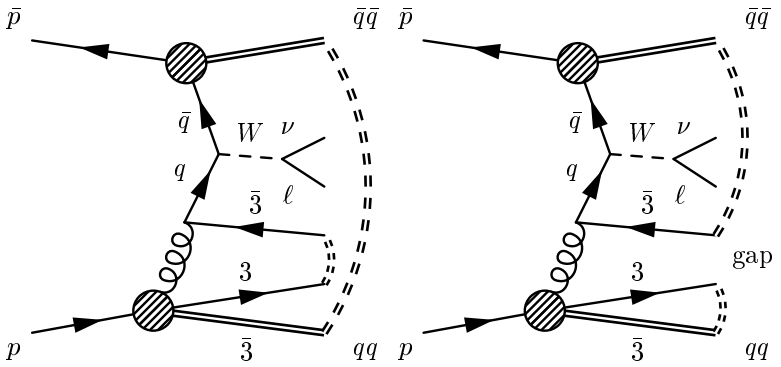

FIG. 4. Production of W (decaying leptonically) in a $p\bar{p}$ collision with string topology (double-dashed lines) before (left) and after (right) a soft color exchange resulting in a rapidity gap.

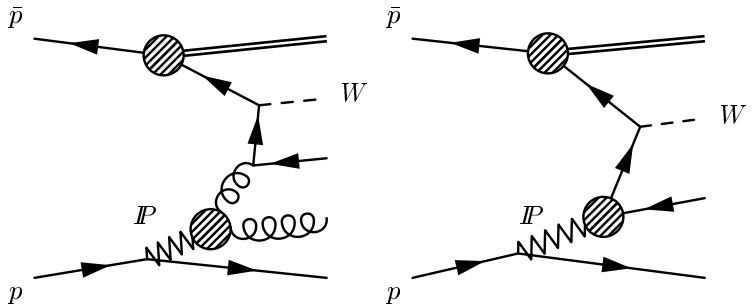

FIG. 5. W production in $p\bar{p}$ in the Pomeron model with a gluon (left) or a quark (right) from the Pomeron entering the hard subprocess.

coupling. Both models have been tuned to describe HERA data. We have mainly used model I, as this describes the Tevatron data better, but we have also tested model II. Still other parametrizations of the Pomeron structure function are available, but using them will not change the results in an essential way.

After having defined our models and described the general framework, we can now turn to the specific diffractive hard scattering processes.

A. Diffractive W production

Diffractive W production has been experimentally observed at the Tevatron by the CDF collaboration at a relative rate $R_W^{\mathrm{CDF}} = (1.15 \pm 0.55)\%$ [17]. Only leptonic decays of the W's are considered here, since they are easier to reconstruct due to a lower background. The interpretation of diffractive W production in the soft color exchange models is illustrated in Fig. 4. In order to have a leading proton, it is necessary to have a gluon-initiated process, i.e., taking a gluon from a beam (anti)proton. The color octet charge of the remnant can

then be neutralized by a soft gluon exchange between this remnant and some other color charge in the event. This may be described in a parton basis as in the SCI model or in a string basis as in the GAL model. In any case, this gives the possibility to produce a small mass leading system, e.g., a single proton, separated by a rapidity gap to the central system containing the W.

In order to produce a leading proton, a parton with not too large energy-momentum fraction x from one beam proton will interact with a parton from the other beam particle. Because of the small energy loss (x) from the leading proton and the large mass of the W, the parton from the other beam hadron will have to be quite energetic and is therefore typically a valence quark. This also implies that the W predominantly emerges in the hemisphere opposite to that of the gap or the leading proton. These effects in our Monte Carlo simulation produce the same correlations of rapidities and W charge as observed by CDF and used in the experimental analysis.

In Pomeron models, on the other hand, W production can be described, as originally proposed and calculated in [44], by the processes in Fig. 5. As discussed above, one folds a Pomeron flux from one of the initial hadrons with a hard Pomeron-proton collision using parton densities in the Pomeron. Since the charge-rapidity correlations are essentially of kinematical origin, they also appear in this model.

The main results of our W simulations are shown in Fig. 6b which shows that the SCI and GAL models reproduce the rate of diffractive W as observed by CDF, whereas the Pomeron model result is far above (about a factor six) and standard PYTHIA is much below the measured value. Here one should remember that the SCI and GAL models are *not* adjusted to these data, but have an absolute normalization which is fixed by the rate of rapidity gaps in DIS at HERA, as discussed in Section III. This ability to reproduce these CDF data is related to the increased rate of high-x_F protons as shown in Fig. 6a. The Pomeron model, which is only applicable for $x_F \gtrsim 0.9$, overshoots the Tevatron diffractive W rate if taken directly over from its tuning to diffractive HERA data. As discussed in Section II, this problem can be cured by introducing some essential modification of the Pomeron model. Since the Pomeron model only applies in a limited x_F range, the curve in Fig. 6a cannot be normalized to unit area and is instead normalized based on its absolute cross in relation to the other models. Concerning this Pomeron model curve, one should note that it is quite flat. The basic $1/(1-x_F)$ dependence in the Pomeron model is here strongly distorted by the kinematical suppression for $x_F \to 1$ imposed by the W mass. This implies that the cross section for diffractive W, as opposed to inclusive single diffraction, is quite sensitive to the cutoff x_{Fmin}.

As pointed out, the rate of diffractive events may depend on whether they are defined in terms of a gap or a leading proton. This CDF result is based on the observation of a gap, but is essentially equivalent to requiring a leading proton with $x_F > 0.9$. The mild, essentially linear variation of the SCI and GAL model results with x_{Fmin} shown in Fig. 6b, demonstrate that the exact x_{Fmin} value is not crucial; in particular in view of the presently rather large error bars on the experimental ratio R_W.

It is now interesting to investigate how variations in the models affect the results. To start with, we find that there is almost no discernible difference between the results from the two variants of the SCI model, i.e., the one which allows color reconnections between any pair of partons and the one which requires one of the interacting partons to be in the

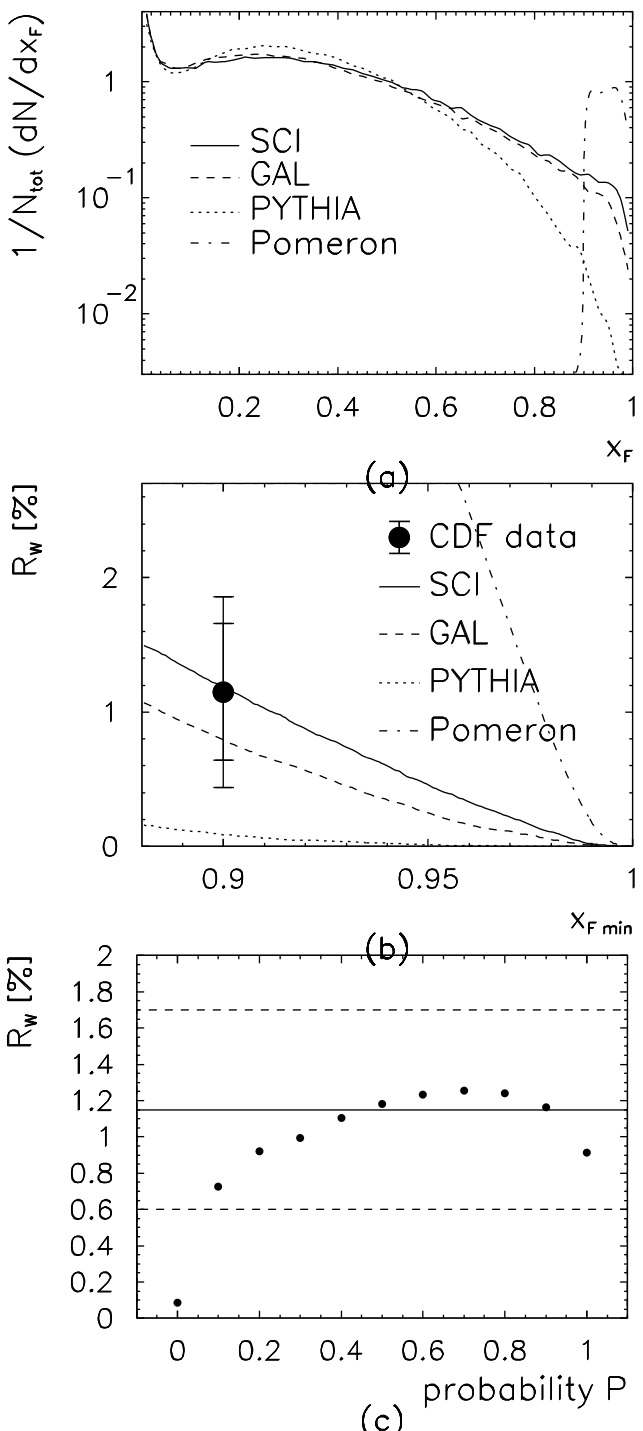

FIG. 6. Results from simulations of W production in $p\bar{p}$ collisions at $\sqrt{s} = 1.8$ TeV using different Monte Carlo models: default PYTHIA, PYTHIA with the soft color interaction models SCI and GAL added, and POMPYT for Pomeron exchange. (a) Distribution in x_F of leading (anti)protons. (b) Relative rate R_W of W events with a leading proton having $x_F > x_{F\min}$. (c) Dependence of R_W on the SCI probability parameter P. The measured value of CDF [17] (with statistical and systematic errors) corresponding to $x_{F\min} = 0.9$ is included as a point in (b) and as lines (central value and errors) in (c).

remnant. This is because practically all rapidity gaps come from reconnections involving a parton in the remnant, representing the color background field. Color exchanges between the more centrally produced partons from the hard scattering do not give rise to large gaps between the central and the leading systems. Consequently, in all simulations in this paper, the standard version of SCI is taken as the one involving at least one parton in the remnant.

One may ask how the diffractive ratio depends on the soft color exchange probability P for the SCI model or P_0 for the GAL model. Qualitatively, if P is large there will be more color reconnections, increasing the rate of gap events. However, an increasing number of color exchanges may also destroy gaps, through the possibility of reconnecting strings 'across' an already formed gap. This behavior is indeed found in the simulation and shown in Fig. 6c obtained using the SCI model. As can be seen, there is only a quite weak dependence on P as long as it does not approach its limiting values 0 or 1. In accordance with earlier studies [12], we take $P = 0.5$ as our value for the SCI probability. For the GAL model, we use the original value $P_0 = 0.1$ [13] as discussed in Section III B.

The improved model for sea quark treatment, which assigns some dynamics to the sea quark partner in the case of scattering off a sea quark in the proton, should be of relevance. The reason is that a sea quark may be viewed as coming from $g \to q\bar{q}$ and thereby be like a gluon-induced process giving diffractive W production as discussed above. As described in Section III C, there are two variants of this sea quark treatment, SQT1 and SQT2. Using one or the other, or neglecting this sea quark treatment, gives somewhat different diffractive W rates as shown in Table II, but the results are all within the experimental error. It could be argued that SQT2 is more correct since it uses sea quark parton distributions to assign momenta, while SQT1 uses pQCD parton splitting functions in the nonperturbative region. Together with the fact that SQT2 gives slightly better agreement with data, this is the preferred version that we use as standard.

The multiple interaction model discussed in Section III C has an important influence on the results. It is clear that in Pomeron models, additional parton-parton scatterings in an event would destroy any gaps, and therefore the existence of a gap would signify that there were no such extra scatterings in the event. In contrast, multiple interactions do not exclude gaps in the soft color interaction models. In fact, the gap ratios shown here for the SCI and GAL models include multiple interactions. The gap rate does depend on the amount of multiple interactions, but switching them off only leads to the somewhat increased gap rate shown in Table II which is still consistent with the observed R_W. Therefore, at this stage of accuracy, the multiple interactions do not present a problem. They must, of course, be included at some level in order to reproduce various characteristics of the underlying event. As discussed above, we have found a slightly increased value of the basic transverse momentum cutoff parameter for these additional parton-parton scatterings to avoid double counting of soft phenomena.

Finally, we have checked the dependence on the choice of parton distribution parametrizations, and we find that the diffractive ratios are slightly smaller (about 15–20%) with CTEQ4L than with CTEQ3L. These variations of the SCI and GAL models result in changes of the diffractive ratios (Table II) which illustrate the uncertainty of the models. We note that these variations are all within the errors of the present experimental results.

In contrast to the soft color exchange models it is, as already emphasized, not possible to take the Pomeron model directly from HERA and use it to reproduce the Tevatron data.

TABLE II. Ratio R_W of diffractive W production obtained from different variations of the models: sea quark treatment (SQT), multiple interactions (MI), parametrization of parton densities in the proton (CTEQ) and in the Pomeron (GS). Results from standard version models are shown in boldface.

Model	R_W (%)
SCI incl. SQT2, MI	**1.2**
" changing to SQT1	1.7
" switching off SQT	0.9
" switching off MI	1.7
" switching to CTEQ4L	1.0
GAL	**0.8**
" switching to CTEQ3L	1.0
Pompyt GS I	**7.2**
" GS II	11.6
Default PYTHIA	0.1

The best result is achieved using model I for the parton densities in the Pomeron, which results in a diffractive W ratio which is six times too large, whereas model II gives a rate about ten times too large (see Table II). Other parametrizations of the Pomeron parton densities exist, but using them will not essentially change this disagreement with Tevatron data which is also compatible with other investigations [8]. We find, however, that some general characteristics such as the η distributions of particles in an event, are the same for PYTHIA with SCI and for POMPYT.

At this point, having examined variations of the models, we make an important observation: the measurement of diffractive W production was only made for the leptonic decay channel $W \to e\nu$. When the W instead decays to quarks, these quarks must also be included in the soft color interactions since, given the short W lifetime, they are produced in a very small space-time region embedded in the color background field of the colliding hadrons. This gives the possibility that reconnections with these decay quarks rearrange the color structure of the event and destroy rapidity gaps. Therefore, the probability for a diffractive event can be lower for hadronic than for leptonic W decays. This effect could be seen as an *apparent* change in the branching ratios of W decays, so that in a diffractive sample of events there will be a higher branching ratio to leptons and a lower branching ratio to hadrons than what is observed in the total, inclusive sample. In Pomeron models on the other hand, no such effect should be present since the hard scattering is independent of the gap-formation process. This has been confirmed by simulations with POMPYT.

The real branching ratios for W are $B(W \to l\nu) = 32.2\%$ and $B(W \to q\bar{q}') = 67.8\%$, and thus $B(W \to l\nu)/B(W \to q\bar{q}') = 0.475$. Now, using the SCI model, but with both the leptonic and the hadronic decay channels of the W included, we find

$$\left.\frac{B^{SCI}(W \to l\nu)}{B^{SCI}(W \to q\bar{q}')}\right|_{\text{diffractive}} = \frac{39\%}{61\%} = 0.63 > 0.475. \tag{3}$$

Thus there are indeed different apparent branching ratios in the biased diffractive W sample.

This is also reflected in the diffractive ratio R_W, which drops from 1.2 to 1.0 when including hadronic W decays.

Naively we would expect the same effect in the GAL model, but this is not observed in our simulations. The reason is that for reconnections with the decay products of the W the price in terms of increased string area is too large. The quarks from the W decay will form a separate color singlet system, which is central in rapidity. Reconnecting this string with a string from a more noncentral parton will typically mean an increase in area, which is strongly suppressed in the model. Therefore we do not observe any shifted apparent branching ratios in the GAL model, only in the SCI model.

The CDF paper [17] also contains a study of the jet structure of diffractive W production. Only 8 out of 34 diffractive events were observed to have a jet giving the ratio 24% , but the relative error is large because of the low statistics. This fraction was used to estimate the quark and gluon content of the Pomeron, and it was found that the measurement was consistent with a quark dominated Pomeron (although the measured value of R_W favors a gluonic Pomeron). An SCI model interpretation is also quite in order, since we have verified that it can reproduce this measured rate of jets in diffractive W events. Here W production with pQCD corrections in terms of next-to-leading order tree level matrix elements and parton showers was employed, however, the description turns out to be equally good using only LO matrix elements and parton showers.

Before moving on to other processes, we will briefly consider diffractive Z production, as this should be qualitatively similar to the W case. This has not been observed experimentally yet since the cross section and branching ratio to leptons are both smaller for Z than for W. We predict diffractive ratios R_Z that are smaller than the corresponding R_W (see Table I): we get $(R_Z/R_W)_{\rm SCI} = 0.83$ and $(R_Z/R_W)_{\rm GAL} = 0.64$. This difference is essentially accounted for by the mass difference; it takes more energy to produce a Z, so there will be less energy available for the leading proton, which will on average have a lower x_F. Thus R_Z will be lower than R_W. We have checked this by a simulation where the Z mass was set equal to the W mass, resulting in a ratio consistent with unity for SCI. We find similar results in the Pomeron model, as expected based on general kinematical mass effects.

In the GAL model, however, the suppression of Z compared to W is larger. Simulating with the GAL model and the Z mass changed to m_W, we get $(R'_Z/R_W)_{\rm GAL} = 0.8$. Hence the larger mass is not the whole reason. The difference between the SCI model and the GAL model is larger for Z than it is for W. This gives an indication that the dependence on the hard scale is different between the two models, as will be discussed in more detail later.

To summarize this subsection, we have demonstrated that the SCI and GAL models can indeed reproduce experimental data on diffractive W production, while the Pomeron model cannot without modifications. We have also studied some variations of the models, and found that the 'best model' is the same model as the one used to reproduce diffractive HERA data, namely, SCI or GAL together with the new model for sea quark treatment (SQT2), but here also with the multiple interaction model necessary for $p\bar{p}$ collisions.

We have also pointed out some differences between the SCI, GAL and Pomeron models, which could be used to experimentally discriminate between them. An interesting such observable is the phenomenon of different apparent W branching ratios in diffractive events.

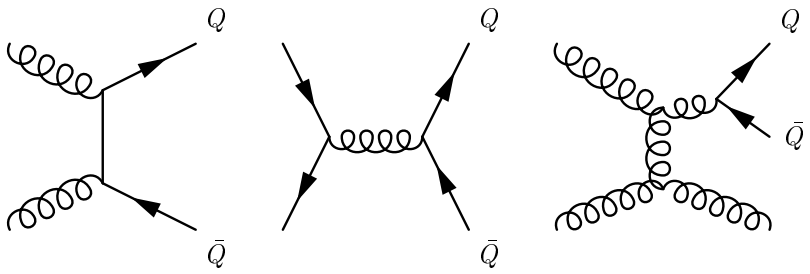

FIG. 7. Examples of pQCD processes for $Q\bar{Q}$ production: the left and middle diagrams show the two leading order (α_s^2) processes and the right diagram shows the most important next-to-leading order (α_s^3) diagram.

B. Diffractive beauty production

CDF has also measured diffractive $b\bar{b}$ production in terms of open beauty in events with rapidity gaps, defined in the same way as in the W case. The resulting ratio of diffractive beauty production is $R_{b\bar{b}} = (0.62 \pm 0.25)\%$ [18].

In contrast to W production, the description of heavy quark production needs to include also higher order diagrams. In leading order (LO) pQCD heavy-quark production occurs through $gg \to b\bar{b}$ and $q\bar{q} \to b\bar{b}$, Fig. 7ab. However, higher order processes involving gluon splitting $g \to b\bar{b}$ are important. For example, the process $gg \to gb\bar{b}$ illustrated in Fig. 7c gives a large contribution because it is an α_s correction to the large cross section for gluon scattering ($gg \to gg$). Matrix elements with explicit heavy-quark mass are available up to next-to-leading order (NLO), but still higher orders may contribute at collider energies. These can only be taken into account through the parton shower (PS) approach which, although being approximate, has the advantage of resumming leading logarithms to all orders.

We therefore investigate beauty production both in leading order and in higher orders (HO) using PYTHIA. The LO matrix elements include the b-quark mass $m_b = 4.5$ GeV. The higher orders are obtained through $g \to b\bar{b}$ in the parton showers added to all LO $2 \to 2$ QCD processes, except those producing $b\bar{b}$. The LO and HO contributions can then be added with their respective cross section weights. The higher orders are tree level diagrams, whereas virtual corrections are not taken into account in this approximation.

The diffractive ratios obtained in this way are listed in Table I and are plotted as functions of $x_{F\,\mathrm{min}}$ in Fig. 8. The separate LO and HO contributions in the figure show that the LO gives a larger gap ratio, but the HO gives a larger contribution to the total cross section. In contrast to W production, GAL here gives a larger gap ratio than SCI and is not in very good agreement with the experimental value. The SCI model gives excellent agreement as usual, whereas the Pomeron model is a factor 15 too large compared to the measurement.

Here we again note that the GAL model has a different energy dependence, larger ratios for smaller hard scales and smaller ratios for larger hard scales, as compared to the SCI model. This was already seen for Z production and we here anticipate the results from

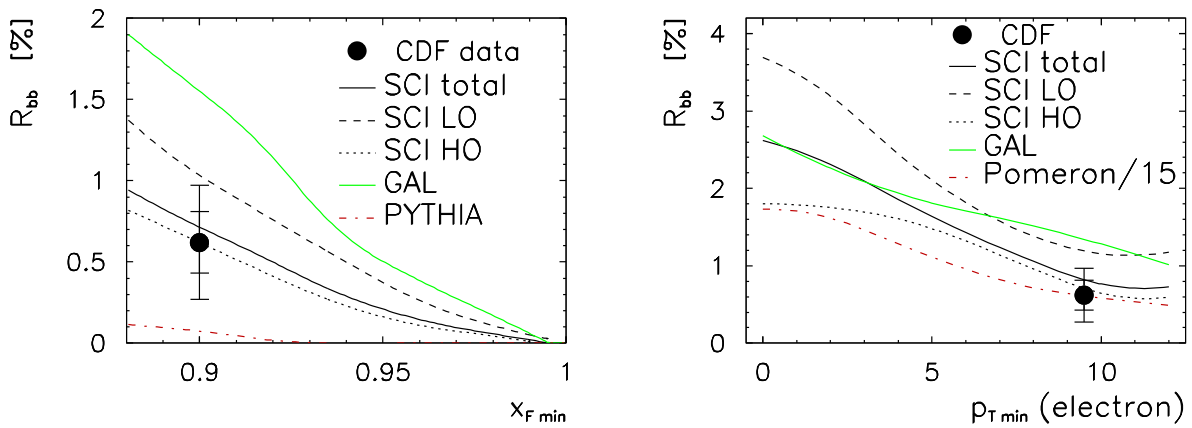

FIG. 8. Relative rate of diffractive $b\bar{b}$ production in $p\bar{p}$ collisions at $\sqrt{s} = 1.8$ TeV as a function of (a) the minimum leading proton x_F, and (b) the minimum transverse momentum of the electron from the b-decay. The CDF measurement [18] (with statistical and systematic errors) is compared to different models: default PYTHIA, SCI with leading order and higher order contribution, GAL and in (b) also Pomeron exchange in POMPYT scaled down by a factor 15.

Sections IV C and VI and observe that the same holds for diffractive dijets and J/ψ.

The experimental observation of B mesons is based on electrons from their decay. One requires these electrons to have a transverse momentum larger than $p^e_{\perp\min} = 9.5$ GeV. This is an important point, since we find that the diffractive ratio $R_{b\bar{b}}$ depends on the value of $p^e_{\perp\min}$, as shown in Fig. 8. The three SCI curves shown (LO, HO, and total) all have the same slopes. The Pomeron curve also has the same slope, but as the absolute normalization is a factor 15 too large, it has been correspondingly rescaled in the figure. The GAL curve is at the same level as the SCI model for small $p^e_{\perp\min}$, but its slope is smaller such that it overshoots the experimental data point. This different slope of the GAL model is again a manifestation of its different scale dependence.

This dependence on $p^e_{\perp\min}$, which is effectively a requirement on the transverse momentum of the $b(\bar{b})$ quark, can arise from an interplay of several effects. First, a higher $p_\perp$ requires larger momentum fractions taken from the colliding protons, which means less energy left for leading protons. Second, with higher $p_\perp$ the incoming and outgoing partons radiate more, thus filling gaps. It is not a priori clear how the underlying event affects this, but we have found that multiple interactions do not change the slope of the curves, only the normalization. Given these effects, one should realize that the measured diffractive beauty ratio might be biased towards a lower value given the requirement of a high-$p_\perp$ electron.

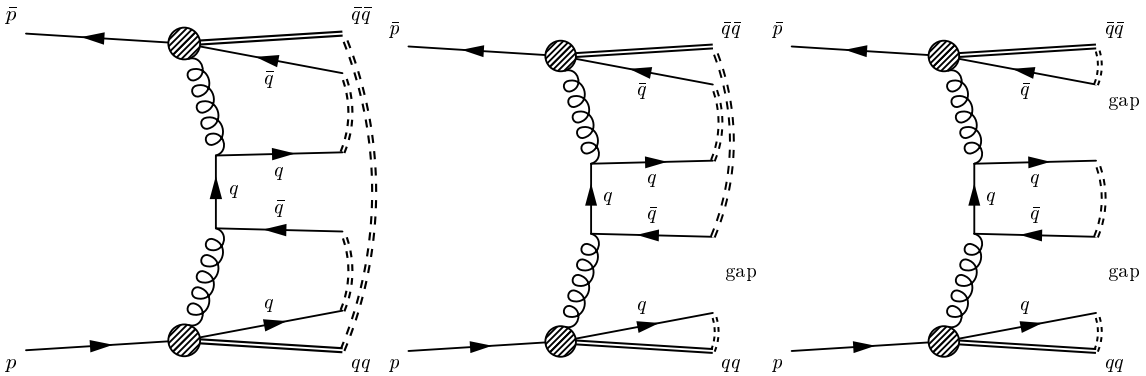

FIG. 9. Dijet production in $p\bar{p}$ collisions with string topologies (double-dashed lines) before and after soft color interactions resulting in events with one gap (leading particle) and two gaps (leading particles).

C. Diffractive dijet production

The process originally considered when introducing the concept of diffractive hard scattering was jet production in high energy hadronic interactions [5]. The transverse momentum ($p_\perp$) or transverse energy (E_T) of the jets provides the hard scale necessary for the study of diffraction based on a firm underlying parton picture. The experimental discovery by UA8 of hard scattering phenomena in diffractive scattering was also in terms of events with a leading proton and high-$p_\perp$ jets at the CERN $p\bar{p}$ collider [45]. Additional UA8 data [46] gave important results, which were mainly interpreted in terms of the Pomeron model resulting in hard parton density distributions in the Pomeron.

Diffractive dijet production has also been observed by the CDF and DØ experiments at the Tevatron. Initially, CDF observed [19] events with high transverse energy jets ($E_T > 20$ GeV) and a gap in the rapidity region opposite to the dijets in $p\bar{p}$ collisions at $\sqrt{s} = 1800$ GeV, while DØ has reported [20] observation of events with a similar topology ($E_T > 12$ GeV and $E_T > 15$ GeV) at the two center of mass energies $\sqrt{s} = 630$ and 1800 GeV, respectively. The analyses are quite analogous to that for diffractive W discussed above, with the observed gap equivalent to a leading proton with $x_F > 0.9$.

This kind of events occurs naturally in the soft color exchange models as illustrated in Fig. 9. Applying the SCI and GAL models to jet production in PYTHIA, described by leading order QCD $2 \to 2$ scattering processes with parton showers added for higher orders, results in a good description of the observed diffractive dijet ratios R_{jj}, as shown in Table I and Fig. 10. We emphasize that it is exactly the same SCI and GAL models as used for diffractive W and $b\bar{b}$ above, only the hard subprocess has been changed. We have investigated the dependence of the results on the reconnection probability P, $p_\perp^{\min}$ in the multiple interaction model, different aspects of the sea quark treatment, and arrived at the same conclusions as for the W case in Section IV A.

The other models cannot reproduce the measured R_{jj}; default PYTHIA is far below data (Fig. 10) and the Pomeron model is above (not shown explicitly).

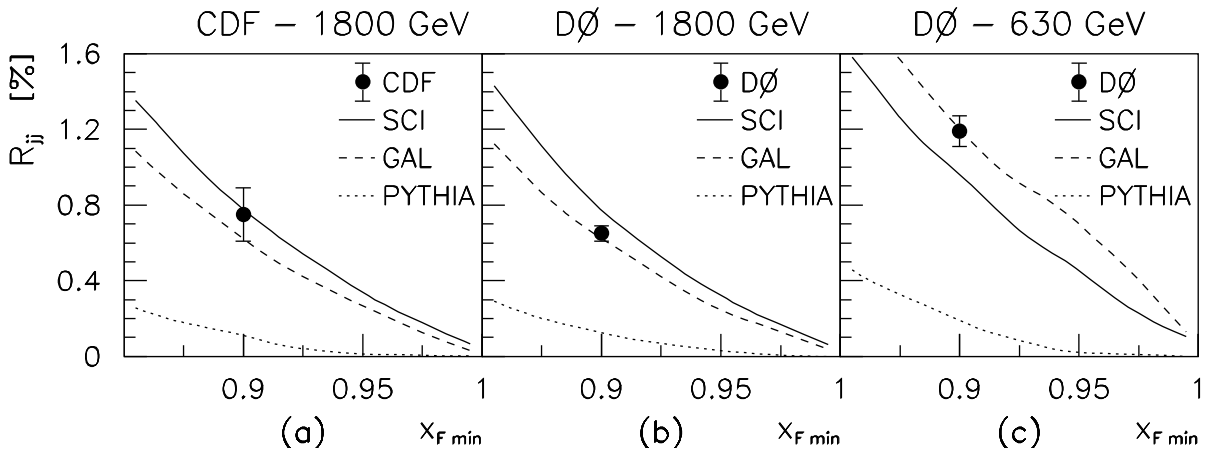

FIG. 10. Relative rate of diffractive dijet production in $p\bar{p}$ collisions as a function of $x_{F\,min}$, the minimum momentum fraction of the leading proton; (a) CDF [19] and (b,c) DØ [20] results at different cms energies are compared to model results (default PYTHIA, SCI and GAL).

CDF has recently presented a new sample of diffractive dijet events, where the signature of diffraction is a leading antiproton observed in Roman pot detectors [10]. The reported results are based on events with antiprotons in the range $0.905 < x_F < 0.965$ and two jets with $E_T > 7$ GeV. Since this offers a new testing ground for the models, we have investigated the production of dijet events with a leading antiproton and compared the results of the models with the observed CDF data. We note that CDF uses the variable ξ to denote the antiproton fractional momentum loss, which is related by $x_F = 1 - \xi$ to the variable x_F consistently used in this paper.

In Fig. 11 we compare characteristic features of the dijet systems in our models and in data. The data show that the E_T distribution of the diffractive sample falls steeper than that of the nondiffractive sample. This behavior is present in both the SCI and GAL models, although the exact shape is not very well reproduced. This may be related to a mismatch between our jet reconstruction procedure and the experimental one, or PYTHIA being limited to leading order matrix elements without next-to-leading order corrections for the basic jet cross section. The rapidity distribution of the jets is in the diffractive sample shifted into the hemisphere opposite to the leading antiproton, a characteristic which is well described by both models, see Fig. 11b for the case of SCI.

CDF has furthermore extracted the ratio of diffractive to nondiffractive dijet events as a function of the momentum fraction x of struck parton in the antiproton. This x can be evaluated from the transverse energy and rapidity of the jets using the relation

$$x = \frac{1}{\sqrt{s}} \sum_{j=1}^{2 \text{ or } 3} E_T^j \; e^{-\eta^j} \tag{4}$$

where the sum includes the two leading jets, plus a third jet if it has $E_T > 5$ GeV. In Fig. 12a we compare their data with the results from the models. The Pomeron model overshoots

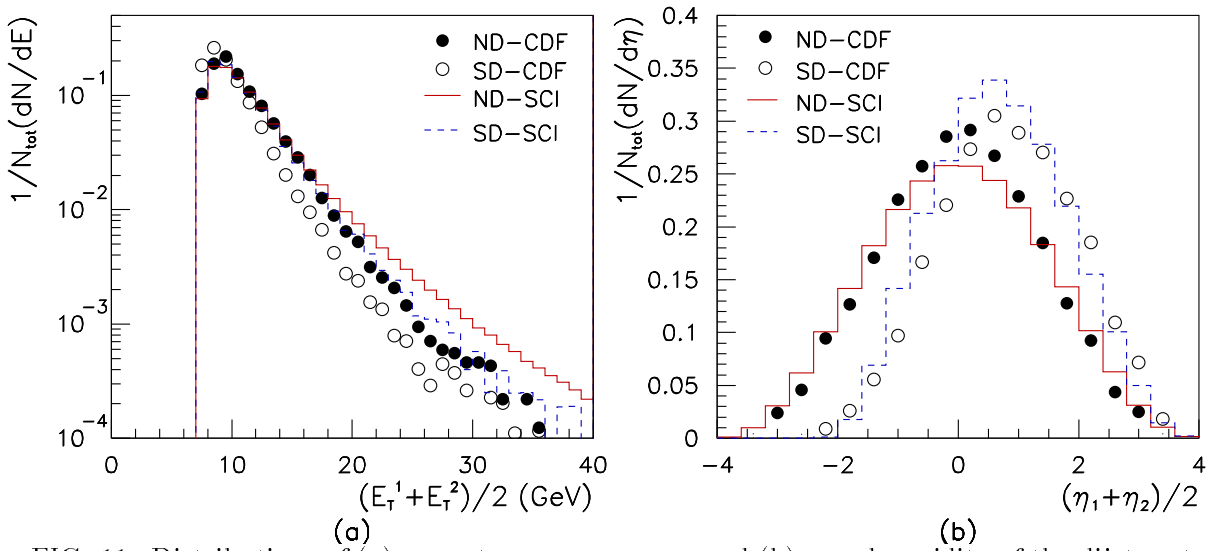

FIG. 11. Distributions of (a) mean transverse energy and (b) pseudorapidity of the dijet system in nondiffractive (ND) and single diffractive (SD) $p\bar{p}$ events at $\sqrt{s} = 1.8$ TeV. The points are CDF [10] data and the histograms are PYTHIA with the soft color interaction (SCI) model added.

the data by an order of magnitude, while default PYTHIA is too low by a similar factor. The soft color exchange models give a fairly correct description, reproducing the overall behavior and giving the correct total ratio. Going into finer details, we note that as x_F approaches unity ($x_F > 0.965$), the slope of this ratio with x becomes more steep in the models (as seen in Fig. 12a, where this contribution is included in the full curve). This behavior seems not to be quite in accord with CDF results, which indicate a constant slope as x_F varies [10]. This dependence in the model is mainly due to the details of the remnant treatment, which affect the steepness of the ratio.

The measurement of the leading antiproton provides a test of exactly how the beam particle remnant is handled in the model. In order to explore this we have investigated the effects of the alternative remnant handling procedures available in PYTHIA. Since diffractive events arise dominantly in the SCI and GAL models from gluon-induced processes, the remnant typically contains the three valence quarks. As described in Section III C, this remnant is split into a quark and a diquark taking energy-momentum fractions χ and $1-\chi$, respectively. The probability distribution $\mathcal{P}(\chi)$ cannot be deduced from first principles, but is given by some parametrization. As our standard choice we use $\mathcal{P}(\chi) \sim (1-\chi)$, giving in the mean one third of the remnant energy-momentum to the quark and two thirds to the diquark. We have also tried other parametrizations, in particular the parton distribution-like form $\mathcal{P}(\chi) \sim \chi^{-1}(1-\chi)^3$. The antiproton x_F spectra obtained are shown in Fig. 12b. The SCI and GAL results are quite similar, but both depend significantly on this remnant treatment. Of course, the main effect in Fig. 12b is the large increase of antiprotons at large x_F when going from default PYTHIA to the SCI or GAL model resulting in an overall

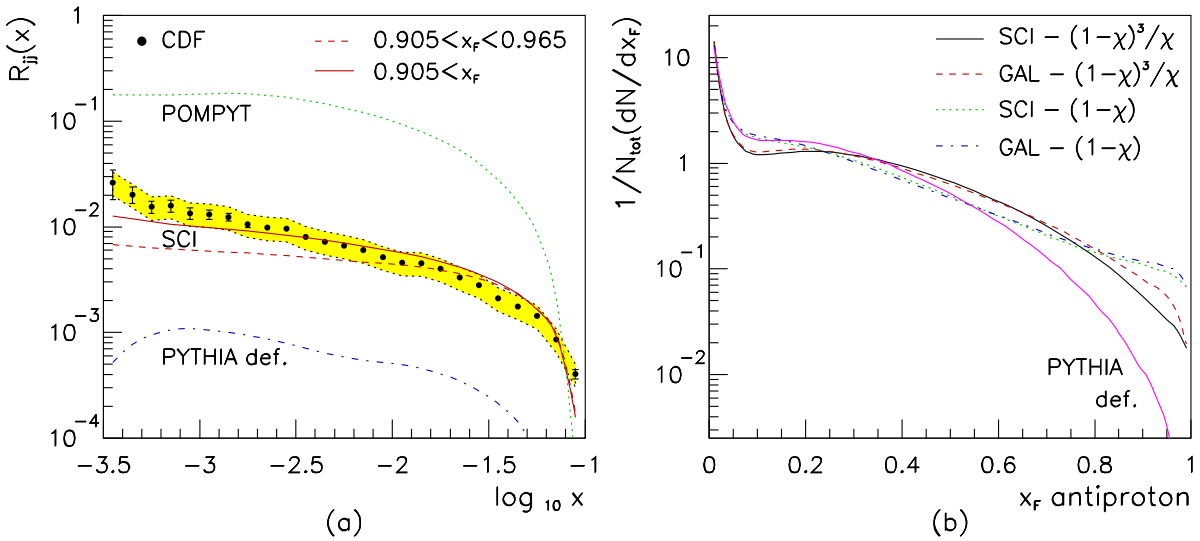

FIG. 12. (a) Ratio of diffractive to nondiffractive dijet events versus momentum fraction x of the interacting parton in $\bar{p}$. The points are CDF data [10] and the shaded band shows the $\pm 25\%$ systematic normalization uncertainty. The curves are from the POMPYT Pomeron model, default PYTHIA and the SCI model (for two x_F regions). (b) Distribution in x_F of the leading $\bar{p}$ from default PYTHIA and the soft color exchange models (SCI, GAL) with varied modeling of the remnant.

description of the diffractive rates. The finer details of the diffractive events will, however, depend on the details in the modeling of the remnant.

Summarizing the investigation of diffractive dijets, the soft exchange models do a very good job in reproducing the overall ratios of diffractive to nondiffractive dijet production. They also give a good agreement with the kinematical distributions observed for this type of events. However, some detailed results depend on the treatment of the proton remnant in the Monte Carlo. The new diffractive Tevatron data based on a leading antiproton provide additional tests of the models.

V. DPE – 'DOUBLE LEADING PROTON EVENTS'

Related to single diffraction are events with *two* leading protons with associated gaps. These protons are at the opposite extremes in phase space, i.e., at $x_F \to +1$ and $x_F \to -1$, and their associated gaps are in the forward and backward rapidity regions, respectively. In the Regge framework these events are described by a process where the two beam protons each emit a Pomeron. These Pomerons then interact, producing a central system which is separated in rapidity from the two quasi-elastically scattered beam protons. This class of events has therefore been called double Pomeron exchange (DPE). This nomenclature is, however, based on an interpretation in a certain model and it would be better to classify

TABLE III. Rates of DPE dijet events in data compared to SCI and GAL models; relative to single diffractive dijet events and absolute cross section.

	$\tilde{R}_{SD}^{DPE}$ [%] [a]	σ^{DPE} [nb]
CDF [22]	0.80 ± 0.26	$43.6 \pm 4.4 \pm 21.6$
SCI	0.54 ± 0.05	5 [b] – 25 [c]
GAL	0.44 ± 0.05	6 [b] – 40 [c]

[a] Calculated per unit $x_F = 1 - \xi$ of leading proton.
[b] Leading proton in $0.97 < x_F < 0.99$.
[c] Only gap requirement on proton side.

them independently of any model and only based on their experimental signature. In order to keep the well established abbreviation DPE, we propose to call them 'Double leading Proton Events'.

These DPE events occur naturally in the soft color interaction models, where the final color string topology may also produce two rapidity gaps as illustrated in Fig. 9c. With one single mechanism for soft color exchanges, different final states will emerge and can be classified in the same way as experimentally observed events: no-gap events, single diffractive events with one gap or a leading proton, or DPE events with two gaps or two leading protons. It is therefore straightforward to extract such events from the Monte Carlo simulations based on the SCI and GAL models.

Both CDF [21] and DØ [47] have observed such DPE events having a dijet system in the central region. They were first identified by two rapidity gaps, one in the forward and one in the backward region. The ratio of two-gap events to one-gap events observed by CDF is well reproduced by the SCI model, as can be seen in Table I. Although DØ has not made such a ratio available, the expectation from the models would be of the same magnitude ($\sim 0.2\%$). Recently, CDF has reported DPE dijet events defined by a leading antiproton and a rapidity gap on the opposite proton side [22]. In the data set of single diffractive dijet events with leading antiproton, they have observed a subset with a rapidity gap on the outgoing proton side at a rate given in Table III. By studying the kinematical correlations between a leading particle and the associated gap, CDF describes the DPE events in terms of a leading proton with $0.97 < x_F < 0.99$, although no such proton is actually observed.

Table III also contains the results of the SCI and GAL models. Applying the leading proton condition strictly results in too low cross sections, but when instead using the more generous gap definition the models reproduce the measured cross section within the errors. This difference between the two approaches illustrates our warning above that leading particle and gap definitions need not be exactly equivalent. In particular, experimental smearing effects may become important when approaching the phase space limit $x_F \to 1$. The absolute cross section is more sensitive to details in the model, such as the remnant treatment and the previously mentioned lack of NLO corrections in PYTHIA may also play a role. With the uncertainties in both data and models in mind, one may conclude that the models give essentially the correct cross section for DPE events.

This discussion illustrates the difficulty to exactly reproduce data in a Monte Carlo model which is ambitious enough to attempt to describe the detailed dynamics of nonperturbative

QCD processes. This problem is accentuated for DPE events, where the gaps and leading particles in both the forward and backward region mean a stronger dependence on the details of the remnant treatment. Using the remnant splitting $\mathcal{P}(\chi) \sim (1-\chi)$ based on simple counting rules, the ratio of DPE to SD events and of SD to ND events gets closer to the measured values than other options for $\mathcal{P}(\chi)$ provided in PYTHIA. The x-dependence of these ratios are shown in Fig. 13. The curve for DPE/SD is obtained with the same leading proton requirement as CDF derived from the observed rapidity gap. The SD/ND ratio differs from the one in Fig. 12a by being calculated per unit $x_F^{\bar{p}}$, which not only changes the normalization but also the slope. The main features of the data are described by the SCI model, but there are discrepancies related to the mentioned problems of the remnant treatment. The main result in Fig. 13 is, however, the breakdown of diffractive factorization, which is quantified by the ratio of SD/ND to DPE/SD ($=0.19 \pm 0.07$) being so clearly different from unity [22]. This important result also emerges from the models.

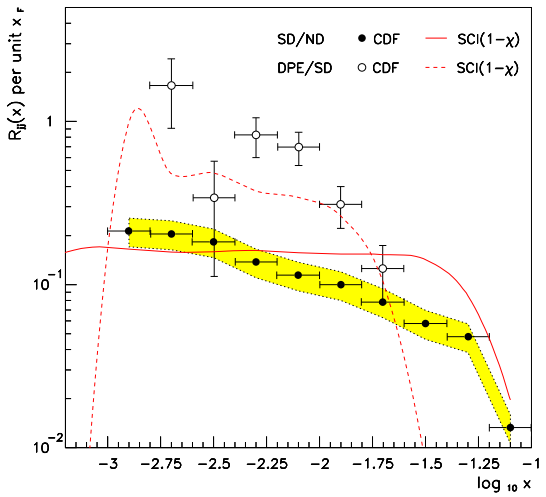

FIG. 13. For dijet event samples, the ratio of DPE to single diffraction (per unit x_F^p) and the ratio of single diffraction to nondiffraction (per unit $x_F^{\bar{p}}$), as a function of the momentum fraction x of the struck parton in p and $\bar{p}$, respectively. The CDF data [22], with statistical errors and a $\pm 20\%$ normalization uncertainty band for SD/ND, is compared to the SCI model using the $(1-\chi)$ parametrization for the remnant treatment in PYTHIA.

After this discussion of the rates of DPE events, we turn to some of their internal properties. Fig. 14 shows some essentials of the jets in DPE events compared to inclusive and single diffractive events. Higher jet multiplicities are clearly suppressed in DPE events compared to the inclusive sample. The slopes of the jet-E_T distributions have a tendency to increase from nondiffractive to single diffractive to DPE events. This can be understood by the limitations on the energy in the hard scattering subsystem due to leading particle effects. The rapidity distribution, which is symmetric around zero for nondiffractive events, is shifted when gap or leading proton conditions are applied on either side. All these features are qualitatively reproduced by the SCI and GAL models. Some discrepancies can, however, be found in the

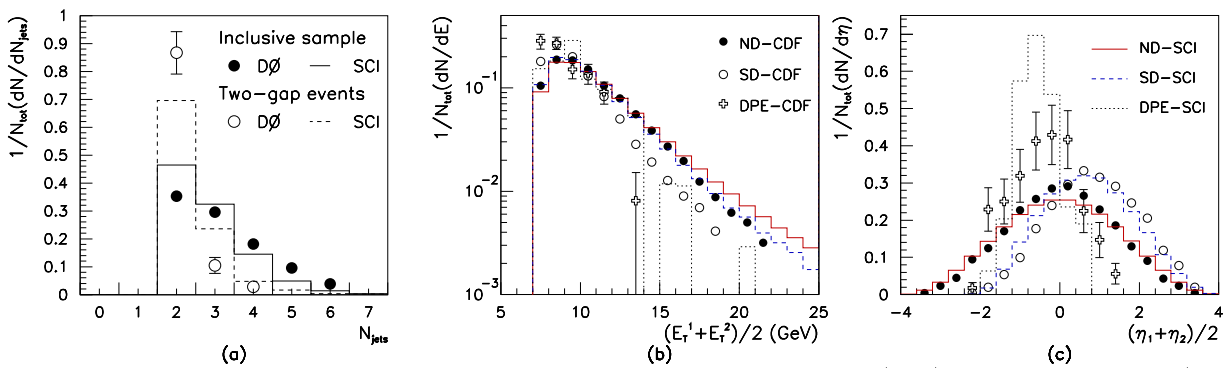

FIG. 14. Comparison of jet properties in inclusive, nondiffractive (ND), single diffractive (SD) and DPE events in $p\bar{p}$ at $\sqrt{s} = 1.8$ TeV; the points are DØ (preliminary) [47] and CDF [22] data and the histograms are from the soft color interaction model. (a) Multiplicity of jets with $E_T > 15$ GeV. (b,c) Distribution of mean transverse energy and pseudorapidity of the two jets with highest E_T (dijet system).

details. The E_T distributions in the models seem to have somewhat too small slopes and higher jet multiplicities are not sufficiently suppressed in DPE events. These deficiencies may be due to a mismatch between data and model regarding the jet reconstruction or the lack of NLO corrections in the hard scattering matrix elements used in PYTHIA.

We have shown in this section how soft color exchange models go beyond their original purpose and explain more than just single diffraction; thus giving a natural description of diffractive events with two gaps or corresponding leading particles. The two leading particles imply an increased sensitivity to the remnant treatment, providing possibilities to test and improve the details of the Monte Carlo model.

VI. DIFFRACTIVE J/ψ PRODUCTION

In the last section it was shown that the soft color interactions can produce two rapidity gaps in the same event and thereby provide a description of DPE. In this section we will demonstrate an even more striking effect where the soft color interactions give rise to two different phenomena in the same event, namely both a rapidity gap and turning a color octet $c\bar{c}$ pair into a singlet giving a J/ψ. The results of our models are predictions to be tested against the data that should appear soon given the very recent observation by CDF of such diffractive J/ψ events. It will be a highly nontrivial result if both the gap formation and the J/ψ production can be well explained with one and the same model for non-pQCD dynamics.

To start with, let us leave diffraction aside and concentrate on the J/ψ production. The main point here is that the soft color interaction, e.g., seen as a soft color-anticolor gluon exchange, can change the color charge of a $c\bar{c}$ pair. A sizable fraction of the large cross section for pQCD production of color octet $c\bar{c}$ pairs can then be turned into color singlet

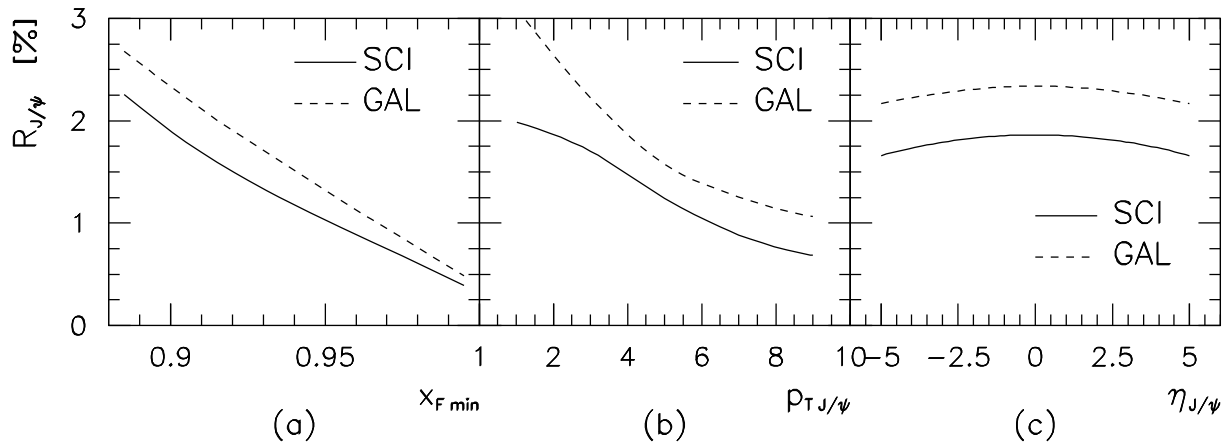

FIG. 15. Predictions of the SCI and GAL models for the ratio of diffractive to inclusive J/ψ production in $p\bar{p}$ at $\sqrt{s} = 1.8$ TeV as a function of (a) $x_{F\,min}$ of the leading proton, (b) the transverse momentum, and (c) the rapidity of the J/ψ ($x_{F\,min} = 0.9$ in (b,c)).

$c\bar{c}$. These will form onium states when their invariant mass is below the threshold for open charm production. It is a remarkable fact [23] that exactly the same SCI model that was used above, reproduces the observed cross sections of high-$p_\perp$ charmonium and bottomonium in $p\bar{p}$ at the Tevatron. Since these cross sections are factors of ten larger than the prediction of conventional pQCD in terms of the color singlet model, where the $c\bar{c}$ is produced in a singlet state, they need a radically new explanation.

The production of charmonium states in fixed target hadronic interactions at different energies can also be described by these kinds of soft color interaction models, as demonstrated in [48]. Furthermore, elastic and inelastic photoproduction of J/ψ at HERA has been investigated from the perspective of soft color exchanges [49]. Although SCI and GAL show good agreement with data for the energy dependence of the cross section, the normalization is uncertain since these models are based on leading order matrix elements. The results are, therefore, sensitive to the choice of factorization and renormalization scale, and in the elastic case, the treatment of the proton remnant.

Given this success of soft color interaction models to describe inclusive heavy quarkonium production, we now turn to diffractive J/ψ production at the Tevatron. The predictions of the SCI and GAL models are shown in Fig. 15. The ratio of diffractive to nondiffractive J/ψ events is in the range 1–2%, depending on $p_\perp$ and η of the J/ψ. This predicted ratio seems to be in agreement with the recent preliminary CDF result [50] of $(0.64 \pm 0.12)/\mathcal{A}$, where $\mathcal{A} \sim 0.4$ is an estimated rapidity gap acceptance. These diffractive events are experimentally defined as events with a rapidity gap and we have performed the analysis similarly to the aforementioned hard processes with a rapidity gap.

For production of $c\bar{c}$ with appropriate invariant mass to form J/ψ, we found that higher order contributions are very important, which was also demonstrated in [23]. The leading order production through $gg \to c\bar{c}$ and $q\bar{q} \to c\bar{c}$ (Fig. 7 a,b) are included through massive matrix elements, while the higher order tree level contributions are taken into account ap-

proximately through the parton shower approach (main contribution in Fig. 7c). LO and HO give the same ratio of diffractive to nondiffractive J/ψ when considered independently, but the HO mechanism gives a higher absolute cross section and therefore dominates the diffractive J/ψ events.

To conclude, we find that the ratio of diffractive to nondiffractive J/ψ predicted in the SCI and GAL models seems to be in agreement with expectations based on recent preliminary experimental results. This shows that the same soft color interaction mechanism can be used to describe both gap formation and quarkonium production, even occurring in the same event!

VII. CONCLUSIONS

A proper understanding of nonperturbative QCD has not yet been possible based on rigorous theory. The development of phenomenological models is therefore a useful approach. By considering soft effects in hard scattering events one can have a firm basis in terms of a parton level process which can be calculated in perturbation theory. Below the cutoff for the perturbative treatment, further interactions occur abundantly because of the large coupling α_s at small scales. The problem is then to model these soft interactions properly. The soft interactions can have large effects on the hadronic final state. This was demonstrated in Fig. 2, where frequently occurring large rapidity gaps on the parton level were filled through the hadronization process resulting in a strong, exponential suppression of large gaps at the hadron level. Conventional hadronization models, like the Lund string model, have a substantial theoretical input and describe very well many aspects of the hadronic final states. Nevertheless, they are still not derived from fundamental QCD theory, but are of phenomenological character and depend on which data have been considered when constructing them. The models may therefore need the introduction of new aspects or new dynamics as other data or new observations are considered.

The soft color interaction approach investigated in this paper is an example of such new dynamics. We have argued that these interactions are a natural part of the process in which bare perturbative partons are dressed into nonperturbative ones and of the formation of color flux tubes between them. In the SCI model this may be viewed as the perturbatively produced partons interacting softly with the color medium of the proton as they propagate through it. Interactions of a color charge with a color background field is a more general problem which has been investigated using other theoretical approaches and received increasing interest in recent years. Examples of effects considered are large K-factors in Drell-Yan processes and synchrotron radiation of soft photons [51] as well as diffractive DIS in a semiclassical model [52]. The new approach to diffraction in [28] may also be possible to interpret in a soft color interaction scenario.

Our phenomenological approach is formulated in terms of the SCI and GAL models which are added to the well-known Monte Carlo programs LEPTO and PYTHIA. A new stage of soft color interactions is introduced after the conventional perturbative processes, described by matrix elements and parton showers, but before applying the standard Lund string hadronization model. The SCI model is formulated in a parton basis, with soft color exchange between quarks and gluons, whereas the GAL model is formulated in a string

basis, with soft color exchange between strings. In both cases, this causes a change of the color string topology of the event such that another hadronic final state will result after hadronization. These fluctuations will sometimes result in a region where no string is stretched giving a rapidity gap after hadronization. In both models there is only one new parameter, giving the probability for such color exchanges. The value of this parameter is chosen such that the rate of diffractive rapidity gap events observed in DIS at HERA is reproduced.

The main result of this paper is that the same soft color interaction models, using the same value for this single new parameter, give a good description of the single diffractive hard scattering phenomena observed at the Tevatron: W, dijets and beauty mesons. Also the observed rate of double leading proton events (DPE), conventionally interpreted as double Pomeron exchange, is well reproduced by the SCI and GAL models. Here, the same soft color interaction mechanism produces two leading protons with associated rapidity gaps in the same event and it is a nontrivial result that the correct rate of DPE events are produced.

Another, even more striking effect of two observables in the same event being explained with the soft color interaction mechanism is diffractive J/ψ production. Here, both a rapidity gap is produced and a color octet $c\bar{c}$ pair is turned into a color singlet such that a charmonium state can be produced. As a result we have predicted a rate of diffractive J/ψ production which seems to be in good agreement with the recent preliminary CDF result. Data on inclusive charmonium and bottomonium production (without gap requirements) are also reproduced, as demonstrated in [23] for the case of high-$p_\perp$ J/ψ, ψ' and Υ at the Tevatron and in [48] for J/ψ and ψ' production at fixed target energies.

Diffractive events at the Tevatron were first obtained based on the observation of rapidity gaps. CDF has also obtained samples defined by measured leading antiprotons in their Roman pot detectors. Compared to the gap definition, this gives consistent results on diffractive rates, but provides additional information. We have used this to test details of the models, in particular the treatment of the hadron remnant which is poorly constrained from data. Here, one has to address issues like the treatment of a complex remnant containing several partons and the hadronization of systems with small invariant mass.

Comparing the different diffractive hard scattering processes we find a general tendency that their ratio to the corresponding nondiffractive processes decreases with increasing scale ($m_{J/\psi}$, $m_{\perp b}$, $p_{\perp\, jet}$, m_W, m_Z) of the hard process. This behavior arises naturally in the models due to two effects. The first is the simple kinematical correlation that an increased hard scale requires a larger momentum fraction x of the incoming parton, leaving less to the hadron remnant and thereby a reduced probability for a leading proton with large x_F. The second effect is more pQCD parton radiation which can populate rapidity regions such that no gap is formed. This decrease of the diffractive ratio with increasing hard scale is somewhat stronger in the GAL model than in the SCI model. This is related to the larger cutoff for parton showers in GAL, leaving less room for radiation at lower hard scales in particular. Furthermore, the interaction probability in GAL depends on the invariant masses of parton pairs, making string reconnections from high-$p_\perp$ partons more likely than from low-$p_\perp$ ones. The experimental measurements do not yet have high enough precision to provide any clear conclusions on this scale dependence.

We have also compared the results of the Pomeron model to our models and to data. With Pomeron parton density parametrizations obtained from diffractive DIS at HERA,

the Pomeron model gives diffractive rates at the Tevatron that are clearly too large. The problems of the Pomeron approach have been discussed together with possible modifications, e.g. of the Pomeron flux, to obtain the correct diffractive rates. There are, however, other more detailed observables that may be used to discriminate between the models. An example was here presented in terms of the SCI model giving different apparent branching ratios of the W in the diffractive sample. A $q\bar{q}$ from the W decay will take part in the soft color interactions and affect the probability for gap formation, whereas leptonic W decays will not have this effect. This means that the sample of W events with a gap requirement becomes biased to having more leptonic W decays. So far, diffractively produced W's have only been reconstructed through their leptonic decays. Future measurements of hadronic W decays in diffractive events are required to explore this difference of the models regarding apparent branching ratios. We note that this effect will not be present for diffractive J/ψ or beauty mesons, since their life times are long enough that their decay products will be produced outside the color background field of the primary interaction.

New data from Run II at the Tevatron with increased luminosity can give valuable new information and higher precision diffractive data. These can provide more decisive tests of the models and discriminate between them, perhaps ruling out some model. In any case, additional data will constrain the models where variations are presently possible, in particular concerning the treatment of the hadron remnants and the formation of leading particles. Application of the models to new processes will also be of interest. We are presently investigating diffractive Higgs production, which will be reported in a forthcoming paper.

Our studies of these soft color interaction models have demonstrated that they are able to reproduce many different phenomena: diffractive hard scattering both in DIS at HERA and at the Tevatron as well as production of heavy quarkonia in hadron interactions at different energies. This is quite remarkable in view of the simplicity of the models, introducing only one new free parameter. It also indicates that these models incorporate some essential features of soft QCD. Therefore, the soft color interaction models should provide guidance for the development of a proper theoretical description of nonperturbative QCD.

ACKNOWLEDGMENTS

We are grateful to A. Edin and J. Rathsman for many helpful and stimulating discussions, and to A. Brandt, K. Goulianos, L. Motyka and C. Royon for discussions and a critical reading of the manuscript.

REFERENCES

[1] G. Ingelman, Diffractive hard scattering, in proc. *Advanced Study Institute on Techniques and Concepts of High Energy Physics*, edited by T. Ferbel (Kluwer academic publishers, 1999), p. 597, hep-ph/9912534.

[2] F. Abe *et al.* (CDF Collaboration), Phys. Rev. Lett. **74**, 855 (1995); *ibid.* **80**, 1156 (1998); *ibid.* **81**, 5278 (1998); B. Abbott *et al.* (DØ Collaboration), Phys. Lett. B **440**, 189 (1998).

[3] R. Enberg *et al.*, to appear in proc. 9th International Workshop on Deep Inelastic Scattering (DIS 2001), hep-ph/0106323, and paper in preparation.

[4] K. Goulianos, Phys. Rept. **101**, 169 (1983).

[5] G. Ingelman and P.E. Schlein, Phys. Lett. **152B**, 256 (1985).

[6] T. Ahmed *et al.* (H1 collaboration), Phys. Lett. B **348**, 681 (1995);
M. Derrick *et al.* (ZEUS collaboration), Z. Phys. C **68**, 569 (1995).

[7] C. Adloff *et al.* (H1 Collaboration), Z. Phys. C **76**, 613 (1997).

[8] L. Alvero, J.C. Collins, J. Terron and J.J. Whitmore, Phys. Rev. D **59**, 074022 (1999); L. Alvero, J.C. Collins and J.J. Whitmore, hep-ph/9806340.

[9] J. C. Collins, Phys. Rev. D **57**, 3051 (1998); [*Erratum-ibid.* D **61**, 019902 (1998)].

[10] T. Affolder *et al.* (CDF Collaboration), Phys. Rev. Lett. **84**, 5043 (2000).

[11] A. Edin, G. Ingelman and J. Rathsman, Phys. Lett. B **366**, 371 (1996).

[12] A. Edin, G. Ingelman and J. Rathsman, Z. Phys. **C75**, 57 (1997).

[13] J. Rathsman, Phys. Lett. B **452**, 364 (1999).

[14] G. Ingelman, A. Edin and J. Rathsman, Comput. Phys. Commun. **101**, 108 (1997).

[15] T. Sjöstrand, Comput. Phys. Commun. **82**, 74 (1994).

[16] B. Andersson, G. Gustafson, G. Ingelman and T. Sjöstrand, Phys. Rep. **97**, 31 (1983).

[17] F. Abe *et al.* (CDF Collaboration), Phys. Rev. Lett. **78**, 2698 (1997).

[18] T. Affolder *et al.* (CDF Collaboration), Phys. Rev. Lett. **84**, 232 (2000).

[19] F. Abe *et al.* (CDF Collaboration), Phys. Rev. Lett. **79**, 2636 (1997).

[20] B. Abbott *et al.* (D0 Collaboration), hep-ex/9912061.

[21] M. Albrow, FERMILAB-CONF-98-138-E (1998).

[22] T. Affolder *et al.* (CDF Collaboration), Phys. Rev. Lett. **85**, 4215 (2000).

[23] A. Edin, G. Ingelman and J. Rathsman, Phys. Rev. **D 56**, 7317 (1997).

[24] A. Donnachie and P.V. Landshoff, Phys. Lett. **191B**, 309 (1987); [*Erratum-ibid.* B **198**, 590 (1987)].

[25] K. Goulianos, Phys. Lett. B **358**, 379 (1995);
K. Goulianos and J. Montanha, Phys. Rev. D **59**, 114017 (1999).

[26] S. Erhan and P.E. Schlein, Phys. Lett. B **427**, 389 (1998).

[27] B. E. Cox, J. R. Forshaw and L. Lönnblad, hep-ph/0012310.

[28] K. Goulianos, J. Phys. G **26**, 716 (2000).

[29] J.C. Collins, L. Frankfurt and M. Strikman, Phys. Lett. B **307**, 161 (1993).

[30] V. A. Khoze, A. D. Martin and M. G. Ryskin, Phys. Lett. B **502**, 87 (2001)
A. B. Kaidalov, V. A. Khoze, A. D. Martin and M. G. Ryskin, hep-ph/0105145.

[31] P.V. Landshoff, in proc. *Workshop on DIS and QCD*, Paris 1995, edited by J.F. Laporte, Y. Sirois (Paris, France, Ecole Polytechnique, 1995), p. 371.

[32] N.N. Nikolaev and B.G. Zakharov, Z. Phys. **C53** (1992) 331;

M. Wüsthoff, Phys. Rev. **D56**, 4311 (1997);
J. Bartels, J. Ellis, H. Kowalski and M. Wüsthoff, Eur. Phys. J. **C7**, 443 (1999);
M. Wüsthoff and A.D. Martin, J.Phys. **G25**, R309-R344 (1999).
[33] V. N. Gribov and L. N. Lipatov, Sov. J. Nucl. Phys. **15**, 438 (1972);
G. Altarelli and G. Parisi, Nucl. Phys. B **126**, 298 (1977);
Yu. L. Dokshitzer, Sov. Phys. JETP **46**, 641 (1977).
[34] A. Edin, G. Ingelman and J. Rathsman, in proc. *Monte Carlo generators for HERA physics*, edited by A.T. Doyle, G. Grindhammer, G. Ingelman and H. Jung, DESY-PROC-1999-02, p. 280, hep-ph/9912539.
[35] A. Edin, G. Ingelman and J. Rathsman, in proc. *Future physics at HERA*, edited by G. Ingelman, A. De Roeck and A. Klanner, DESY 96-235, p. 580.
[36] C. Adloff *et al.* (H1 Collaboration), Eur. Phys. J. **C6**, 587 (1999).
[37] T. Sjöstrand and M. van Zijl, Phys. Lett. **188B**, 149 (1987); Phys. Rev. **D36**, 2019 (1987).
[38] G. J. Alner *et al.* (UA5 Collaboration), Phys. Lett. B **138**, 304 (1984);
G. Arnison *et al.* (UA1 Collaboration), Phys. Lett. **B132**, 214 (1983).
[39] T. Sjöstrand *et al.*, Comput. Phys. Commun. **135**, 238 (2001).
[40] H.L. Lai *et al.* (CTEQ Collaboration), Phys. Rev. **D51**, 4763 (1995).
[41] H.L. Lai *et al.* (CTEQ Collaboration), Phys. Rev. **D55**, 1280 (1997).
[42] P. Bruni and G. Ingelman, DESY-93-187 in proc. International Europhysics Conference on High Energy Physics, Marseille 1993, p. 595;
P. Bruni, A. Edin and G. Ingelman, `http://www3.tsl.uu.se/thep/pompyt/`.
[43] T. Gehrmann and W.J. Stirling, Z. Phys. **C70**, 89 (1996).
[44] P. Bruni and G. Ingelman, Phys. Lett. B **311**, 317 (1993).
[45] R. Bonino *et al.* (UA8 Collaboration), Phys. Lett. B **211**, 239 (1988).
[46] A. Brandt *et al.* (UA8 Collaboration), Phys. Lett. B **297**, 417 (1992); Phys. Lett. B **421**, 395 (1998).
[47] DØ collaboration, Hard Diffractive Jet Production at DØ, presented at *XXIX International Conference on High Energy Physics, ICHEP 98*, July 1998, Vancouver, Canada;
K. Mauritz, Nucl. Phys. (Proc. Suppl.) **B79**, 378 (1999).
[48] C. B. Mariotto, M. B. Gay Ducati and G. Ingelman, Hard and soft QCD in charmonium production, hep-ph/0008200;
M. B. Gay Ducati, G. Ingelman and C. B. Mariotto, Soft and Hard QCD Dynamics in J/ψ Hadroproduction, Uppsala report TSL/ISV-2001-0241 and paper in preparation.
[49] J. Rathsman, in proc. *Monte Carlo generators for HERA physics*, edited by A.T. Doyle, G. Grindhammer, G. Ingelman and H. Jung, DESY-PROC-1999-02, p. 421, SLAC-PUB-8343, TSL-ISV-99-0219.
[50] K. Goulianos, FERMILAB-CONF-99-154-E (1999).
[51] O. Nachtmann and A. Reiter, Z. Phys. C **24**, 283 (1984);
G. W. Botz, P. Haberl and O. Nachtmann, Z. Phys. C **67**, 143 (1995).
[52] W. Buchmüller and A. Hebecker, Nucl. Phys. B **476**, 203 (1996); see also the review in A. Hebecker, Phys. Rept. **331**, 1 (2000).